Version of Record: https://www.sciencedirect.com/science/article/pii/S0272771419304287
Manuscript_f4bec3516670a332c54bcc22871303eb

On the Nature of Tidal Asymmetry in the Gulf of Khambhat, Arabian Sea using the HF Radar Surface Currents

Samiran Mandal[1], Sourav Sil[1], Avijit Gangopadhyay[2, 1, 3], Basanta Kumar Jena[4], Ramasamy Venkatesan[5]

[1]School of Earth, Ocean and Climate Sciences, Indian Institute of Technology Bhubaneswar, India

[2]School for Marine Science and Technology, University of Massachusetts, Dartmouth, USA

[3]Center for Ocean, Rivers, Atmosphere and Land Sciences, Indian Institute of Technology Kharagpur, India

[4]Coastal and Environmental Engineering, National Institute of Ocean Technology, Chennai, India

[5]Ocean Observation Systems, National Institute of Ocean Technology, Chennai, India

Submitted to

Estuarine, Coastal and Shelf Science

First Submission: 7th May 2019
First Revision: 7th September 2019
Second Revision: 24th October 2019

*Corresponding author: Dr. Sourav Sil, Ocean Analysis and Modelling Laboratory, School of Earth, Ocean and Climate Sciences, Indian Institute of Technology Bhubaneswar, Odisha, India- 752050. E-mail: souravsil@iitbbs.ac.in

Abstract

The hourly ocean surface current observations from available High Frequency Radars (HFR) have been analyzed to i) quantify the tidal constituents, ii) investigate the role of the bathymetry on shallow water tides, and iii) identify the nature of tidal asymmetry in the inverted funnel-shaped Gulf of Khambhat (GoKh) on the western shelf of India during May 2012. The HFR observations captured strong currents (~2.0 m s^{-1}), showing significant spring – neap variations. Tidal harmonic analysis of the HFR currents showed that the tidal currents at the mouth are dominated by the M2 constituent with amplitude ~4.5 times higher than that of K1. Among the shallow water constituents, M4 dominates the entire Gulf with significant amplitudes (~10 cm s^{-1}) and gets amplified towards the head of the Gulf (~30 cm s^{-1}), followed by MS4. Comparisons with sea level heights from tide gauges show a higher correlation for the major (>0.97) and shallow water (>0.96) tidal constituents in terms of the order of amplitudes of the tidal constituents. The circulation pattern in the Gulf is predominantly driven by tidal currents, with the total tidal variance being ~90% of the total current variance. The major contributions are from the M2 tidal currents (70-90%), except at the head, where the M4 component contributes significantly up to 40%. The interactions with shallow bathymetry are responsible for the amplification of tidal currents in this converging channel with negligible impact from stratification during May. The harmonic analysis-derived relative surface phase (2M2 – M4) and higher M4/M2 amplitude ratio at the head of the Gulf reveal that the Gulf is highly tidally asymmetric and flood dominant, indicating stronger non-linear tidal distortions in the nearshore regions. A generalized skewness-based analysis confirms the flood-dominance with positive values of a morphology-dependent asymmetry factor and skewness. Two tidal combinations (M2/M4 overtide and M2/S2/MS4 compound tide) are identified as the major contributors to the flow velocity skewness in the GoKh with mixed, mainly semi-diurnal tidal regime.

Keywords: Arabian Sea; Gulf of Khambhat; HF Radar; Flood and Ebb Currents; Tidal Currents; Shallow Water Tides, Tidal Asymmetry.

1. Introduction

The continental shelf along the western coast of India widens towards the north-eastern edge (~250 km off Mumbai coast) of the Arabian Sea (AS), followed by gradual narrowing in the head region (Fig. 1). The shelf further leads into two Gulfs: the Gulf of Khambhat (GoKh, also recognized as the Gulf of Cambay) and the Gulf of Kutch (GoKu), which are regions well-known for significant amplification of tides. The quote below briefly explains the first observations of the strongest tides in the GoKh, which motivated us to analyze the tidal dynamics in this region.

"Recent excavations in the Ahmedabad district of India have revealed a tidal dockyard which dates back to 2450 BC. There is no evidence that the Harappans had enough tidal experience to design and build docks, relating the local tidal movements to the sun and moon. The large twice-daily tides of this region of the Indian Ocean amazed the army of Alexander the Great as it travelled in 325 BC southward along the river Indus towards the sea, as they had only experiences of smaller tides in the Mediterranean Sea" (Pugh, 1987).

Along the continental shelf-to-slope regions, both the baroclinic (internal tides) and barotropic tidal currents have been widely studied around the world ocean, which play a vital role in controlling the various oceanic processes like sediment transports and vertical mixing (Jithin et al., 2017; Subeesh and Unnikrishnan, 2016; Xu et al., 2013). Several studies have investigated the coastal hydrodynamics along the eastern AS using observational datasets. Nevertheless, as they are for short periods and at specific locations, the temporal and spatial variability could not be studied, especially for the Gulf region. The short-term and high-frequency datasets provided information about wind-driven currents (Antony and Shenoi, 1993; Shetye et al., 2008; Unnikrishnan and Antony, 1990; Varkey, 1980) with preliminary insight into tidal constituents (Shenoi et al., 1988, 1994) along the western continental shelf of India.

Analyses using continuous current meter observations over a week indicated the presence of strong semi-diurnal baroclinic and barotropic tidal currents off Goa (Shenoi et al., 1988) and at the mid-shelf of the Mumbai High region (Fernandes et al., 1993). With a yearlong current meter dataset, inter-seasonal variability of M2-driven barotropic semi-diurnal tidal current was investigated, and velocities were estimated to be 1.2 to 1.6 cm s^{-1} in the mid-AS (Shenoi et al., 1992). Recently, inter-seasonal tidal current variability (at both surface and subsurface) along the continental shelf of the west coast of the AS has been investigated using Acoustic Doppler Current Profiler (ADCP)-retrieved observations near Mumbai (Subeesh et al., 2013). They have concluded that M2-driven internal tides are the strongest,

followed by other significant tidal constituents (K1, S2, and O1). The amplitudes of the semi-major axis of M2 ellipses at the northernmost location are ~3 times greater than those at the southernmost location. The strong influence of seasonal stratification on internal tides is also observed. Further, Subeesh and Unnikrishnan (2016) have studied the characteristics of the internal tides and near-inertial waves with a special focus on the continental shelf and slope off Jaigarh (17 ºN), Mumbai, central west coast of India using the same ADCP datasets. Based on "critical topography" estimations and barotropic body force, the deeper part, mid-slope, and shelf-edge of the continental slope are identified as the possible regions for the generation of stronger internal tides.

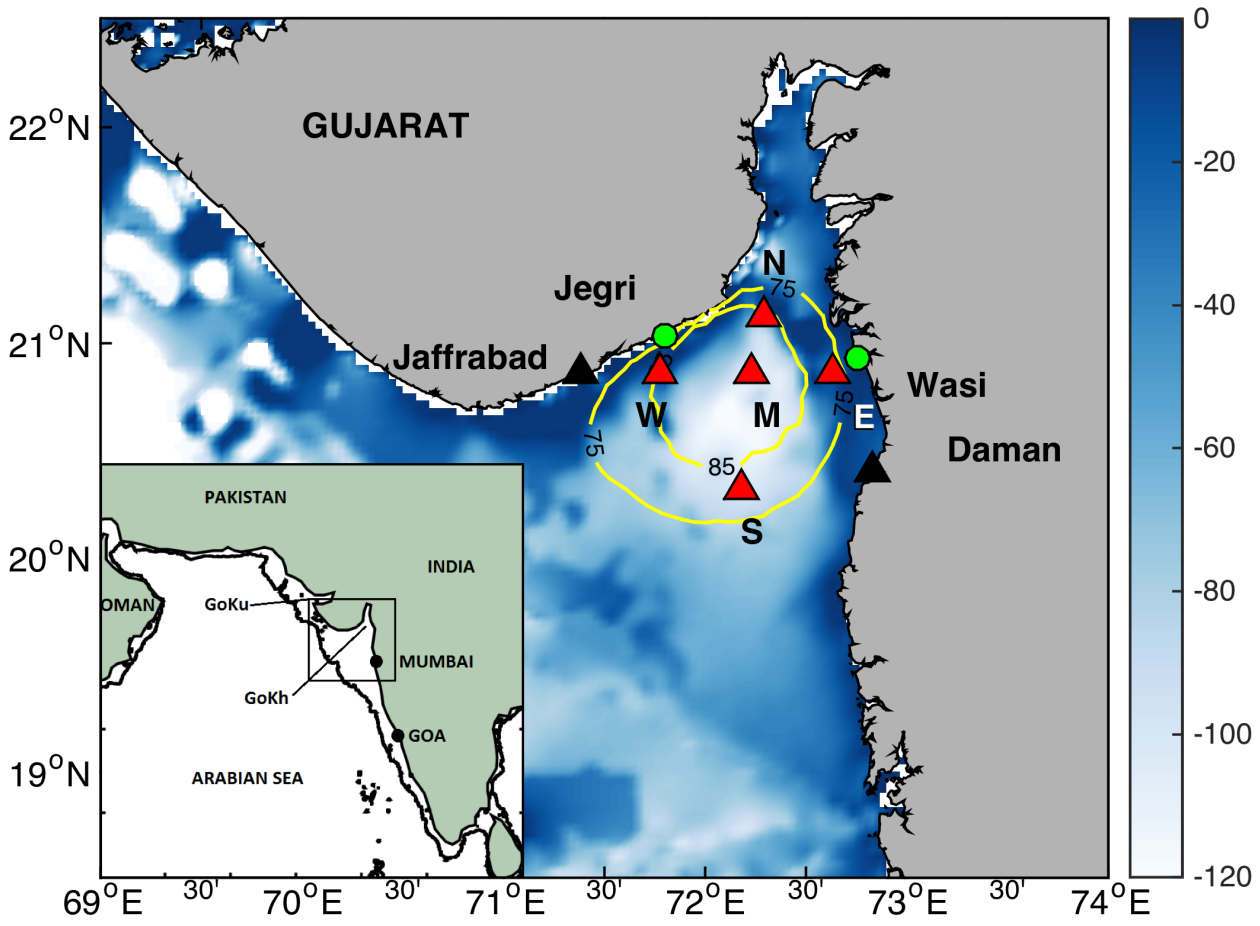

Fig. 1: The data coverage during May 2012 in percentage (%). The yellow contours indicate 75% and 85% data densities. The locations of the comparison points – N (72.29 ºE, 21.13 ºN), W (71.77 ºE, 20.86 ºN), E (72.64 ºE, 20.85 ºN), M (72.23 ºE, 20.85 ºN) and S (72.23 ºE, 20.32 ºN) – are indicated by red triangle symbols. The shaded background denotes the bathymetry from ETOPO2 (color bar in meters). Green dots indicate High Frequency Radar (HFR) stations at Jegri and Wasi Borsi lighthouse, Gujarat, India. The black triangles indicate the tide gauge stations at Daman and Jaffrabad. The inset in the left bottom corner shows the domain of our study with respect to the Arabian Sea. The thick black line is the -200 m isobath indicating the continental shelf.

In GoKh, an observation-based study revealed that surface currents are predominantly tidally induced with speeds up to 3.3 m s^{-1} and are north-northwest (south-southwest) during flood (ebb) tide (Kumar and Kumar, 2010). The zones with distinct bottom frictions have significant influences on the spatial variability of tidal amplitudes and currents throughout the Gulf, which leads to tidal asymmetry (Kumar and Balaji, 2015). A system is referred to as flood dominant or flood asymmetric when the duration of the falling tide exceeds that of the rising tide leading to a larger peak flood current, i.e., the water level rises faster than it falls. It is other way round for ebb dominant systems. Tidal asymmetry is defined as the distortions in durations of rise and fall of water levels (tide duration asymmetry), as well as the distortions in the duration and magnitude of flood and ebb tidal currents (flow velocity asymmetry, FVA) (Friedrichs and Aubrey, 1988). The non-linear tidal distortions in the Gulfs are generally investigated using the amplitude ratio of shallow water tidal constituent (M4) and semi-diurnal tide (M2) and their relative surface phase (2M2 – M4). The major role of the overtides and compound tides on tidal asymmetry inside the Gulfs is in changing the flood and ebb duration within the Gulfs (Friedrichs and Aubrey, 1988). The tidal flow (flood or ebb dominance) is dependent on the relative phase shifting from M4 to M2 (Aubrey and Speer, 1985; Speer and Aubrey, 1985). Earlier studies associated with asymmetry mainly dealt with long-term sea level datasets from tide gauges (Friedrichs & Aubrey, 1988; Guo et al., 2014; Wang et al., 1999) and model simulated surface currents (Gong et al., 2016) using the harmonic analysis approach. However, a limitation of this method is its high sensitivity to the length of the dataset. The adjacent constituents (such as N2) cannot be resolved from the short record lengths. To deal with this limitation, a novel skewness-based method was proposed to characterize tidal asymmetry, even with shorter time series (Nidzieko, 2010). The study has demonstrated and quantified on how a pair of harmonically related tidal constituents affect the skewness. Using the results from Nidzeiko's analysis, Song et al. (2011) have identified distinct combinations of tidal constituents to contribute to asymmetry and further quantify the relative contribution of each one of them to the overall skewness. This method has been applied to the sea-level datasets from the tide gauges at the Skagit river delta, US (Nidzieko and Ralston, 2012), the west coast of Korea (Suh et al., 2014) and Venice Lagoon (Ferrarin et al., 2015).

In the eastern AS, tidal asymmetry in Mandovi and Zuari estuaries along the west coast of India has been analyzed using tide gauge observations as well as model datasets (Manoj et al., 2009). The M4/M2 amplitude ratio exhibits marginal (gradually increasing) tidal distortions in the upstream regions of Mandovi (Zuari) estuary. The higher the amplitude ratio, the stronger is the tidal distortion in Zuari estuary. Similarly, the tidal asymmetry is investigated in the Hooghly estuary using the Advanced Circulation (ADCIRC) and analytical models (Jena et al., 2018). The tidal asymmetry along the GoKh

has not been studied till now, as none of the studies have emphasized on the overtides (M4, S4, M6, M8) and compound tides (MK3, MN4, MS4, 2SM6, 2MS6) variability. So, one of the principal objectives of this study is to investigate the nature of tidal asymmetry in the GoKh using HFR currents applying both the skewness-based approach and harmonic analysis method, as asymmetry plays a significant role in the sediment transport and erosion related studies.

Recently, a pair of High Frequency Radars (HFR) has been installed at Wasi Borsi and Jegri lighthouses, Gujarat (green dots, Fig. 1) by the National Institute of Ocean Technology (NIOT), India, as part of the Indian Coastal Ocean Radar Network (ICORN) (Arunraj et al., 2018; Jena et al., 2019; Mandal et al., 2018a, 2019a, 2019b, 2019c). This study is the first of its kind to focus especially on the extensive utilization of the HFR datasets to explore the high-resolution circulation variability for the spatial quantification of tidal currents and associated dynamics in this Gulf. Moreover, the following scientific questions have been addressed. How do the surface tidal currents, which are primarily set up by the major and shallow water tides vary spatially within the GoKh? How does bathymetry interact with the tidal currents in a funnel-shaped Gulf? And finally, what is the nature of tidal asymmetry in the Gulf? Note that the studies in the BoB were for a straight coast in the different parts of western BoB, while this present study is in a Gulf in the northeastern AS, so the geometry, tidal constituents, and their variability are very different.

The paper is organized as follows: Section 2 briefly describes the hydrography of the Gulf. Section 3 outlines the various datasets and explains the methodology for determining asymmetry using the harmonic analysis and a new skewness-based approach. Section 4 focuses first on the validation of the tidal constituents present in the hourly HFR-derived ocean surface currents with those in the tide-gauge derived sea level datasets at Daman and Jaffrabad. The statistical metrics are then discussed, including the standard measures of center and dispersion. Section 4 also presents the results on the tidal dynamics and outlines the possible reasons for the observed tidal current variability. Section 5 presents the nature of the tidal asymmetry using both the harmonic analysis and the skewness-based approach. Section 6 summarises the major findings with conclusions.

2. The Gulf of Khambhat (GoKh) – Domain, Hydrography, and Tidal Setup

The GoKh on the western shelf of India is an inverted funnel-shaped region with the shallowest bathymetry between the Saurashtra Peninsula and the mainland of Gujarat. The entire bank adjoining the Gulf is surrounded by dense tidal flats, which play a significant role in tidal asymmetry. The rivers like

the Narmada, Tapti, and Sabarmati are the major sources of river discharge during boreal summer (southwest monsoon). Due to the unavailability of *in situ* datasets in the region, the sea surface temperature (SST) from GHRSST and the climatological datasets of temperature and salinity are used to compute stratification (Chatterjee et al., 2012). During May 2012, the westerly winds are observed to dominate throughout the Gulf, with speeds of ~ 5.5 m s^{-1} (Fig. 2a). The SST does not show significant spatial variations within the Gulf during the study period. Fig. 2b shows the vertical structure of temperature (black line) and salinity (red line) at location 'C' (in the domain of interest), indicating constant salinity (~35.94 psu) with negligible stratification. A sharp decline in subsurface temperature (~2 ºC) is observed along the water column (Fig. 2b). Moreover, a highly stratified and stable water column is observed from Brunt–Väisälä frequency (Fig. 2c) during the post-monsoon season (September – November).

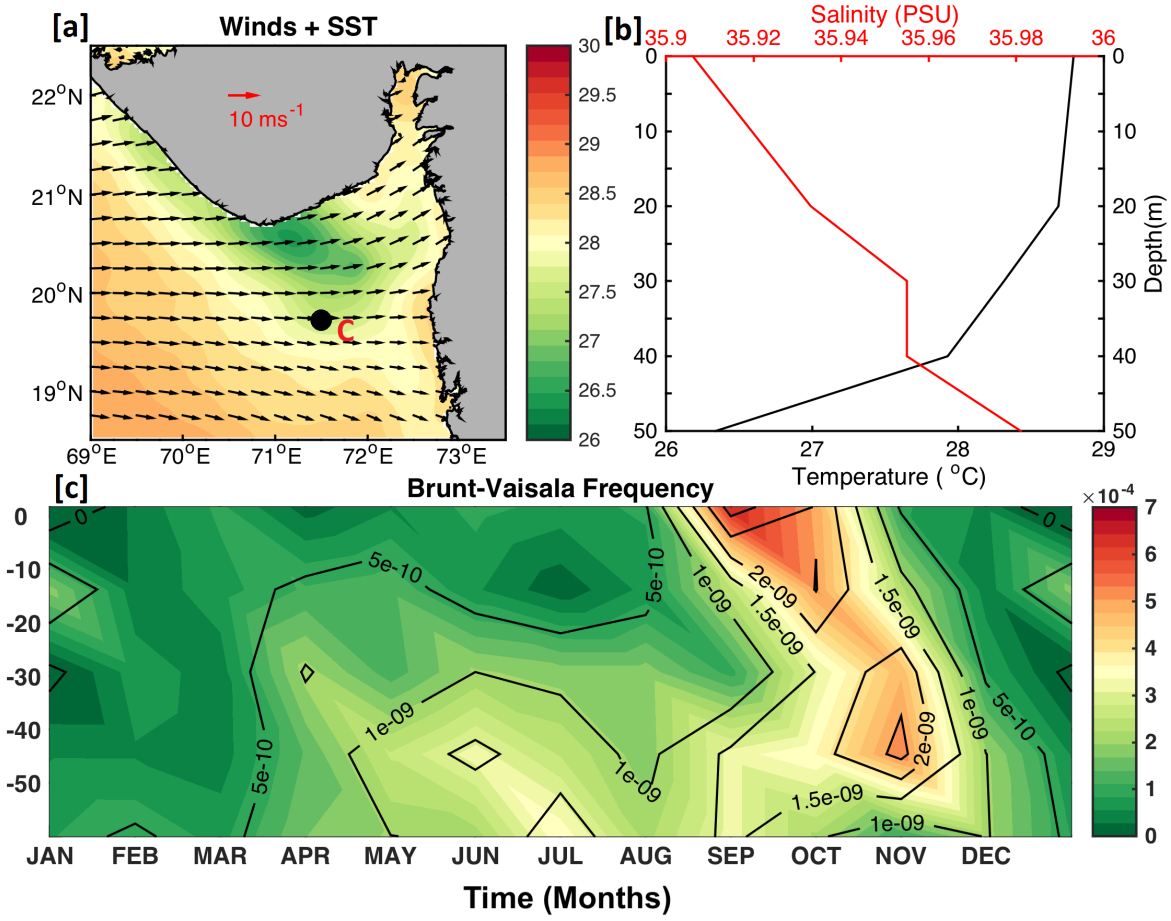

Fig. 2: (a) The monthly averaged surface winds with monthly mean sea surface temperature (shaded) in the GoKh. (b) The monthly climatological vertical profiles of temperature and salinity at location 'C'. (c) The variation of Brunt–Väisälä frequency (N^2) calculated from climatological temperature and salinity datasets (Chatterjee et al., 2012).

The northern part of the Gulf is covered with prominent sand shoals (basically a sandbank). The middle portion of the Gulf, with an extent of ~50 km and bathymetry ranges of ~10-20 m, is highly influenced by the strong currents (Kumar and Kumar, 2010). On the other hand, the southern side of the Gulf is ~230 km wide and shallow (<50 m depth). The characteristics of the tidal regime change from mixed, mainly semi-diurnal to strong semi-diurnal from the southern to the northern part of the west coast. However, the Gulf has the highest tidal range, i.e., 175-275 (45-60) cm for M2 (K1), as compared to other locations along the Indian coastline, which has been reported by Unnikrishnan et al. (1999a), using a barotropic tidal model, and thereby showing the amplification of M2 tides in the Gulf. Later, Nayak and Shetye (2003) quantified this amplification variation to be three times for the semi-diurnal tides from the mouth to the head, whereas the diurnal tides have amplified less. The present study focuses mainly on extracting the spatial distribution of high-frequency tidal variability using the HFR observations and comparison with earlier modeling (Nayak and Shetye, 2003; Unnikrishnan et al., 1999a) and observation-based (Kumar and Kumar, 2010) studies.

3. Materials and Methods

This section comprises of two subsections: (i) a brief technical description of the HFR systems and other datasets, and (ii) methodology used in this work.

3.1. Data

This study presents the analysis of the 2D surface current structure in the GoKh region based on HFR data. For brevity, the measurement accuracy of the HFR systems, and the quality control (QC)/ quality assessment (QA) procedures of the HFR data are briefly described in Appendix A. Several other datasets, which are used in supporting analyses are discussed next, followed by the methodology to determine asymmetry.

3.1.1. High Frequency Radar data

Two radars (SeaSonde HFR Systems, Barrick et al., 1977) are installed along the Gujarat coastline at Wasi Borsi (72.76 ºE, 20.93 ºN) and Jegri (71.81 ºE, 21.04 ºN) lighthouses, and are operating with a frequency of 4.4 MHz, bandwidth of 25 kHz, and cover a maximum range of ~200 km away from the coastline (Jena et al., 2019). This study has been carried out using the hourly QA/QC-ed HFR currents, available at a spatial resolution of ~6 km over a limited region (70.75 – 72.90 ºE, 19.5 – 21.25 ºN) for 31 days during May 2012 with minimum gaps (Arunraj et al., 2018; Mandal et al., 2018b; 2019a;

2019b; 2019c). Key elements of the QA/QC procedure are explained in Appendix A, and a detailed description of these methods can be obtained from the QA/QC manual of ICORN (source: https://www.niot.res.in/documents/HFR_QAQC_doc.pdf).

Cook and Shay (2002) suggested that a minimum period of 29 days is sufficient to resolve the most energetic tidal constituents up to K1 (period of 23.56 hours); therefore, the data length fulfils the requirement of tidal analysis. The data density coverage and location of maximum data availability (shaded) are shown in Fig. 1.

3.1.2 Other datasets

The monthly climatological temperature and salinity (at surface and subsurface) datasets available at a spatial resolution of 1º have been utilized to explain the hydrography of the Gulf (Chatterjee et al., 2012). High-resolution (1/20º) daily SST data are analyzed to investigate the spatial variations of SST within the Gulf (source: http://ghrsst.jpl.nasa.gov). The hourly sea level datasets derived from tide gauges (source: NIOT, Chennai, India) during the same duration of the analysis of the HFR currents (May 2012) at Daman (72.83 ºE, 20.40 ºN) and Jaffrabad (71.38 ºE, 20.86 ºN) are used for comparison with the HFR-derived surface currents at tidal scale. The ETOPO2 (Earth Topography 2) bathymetry dataset (spatial resolution of ~3 km) is used to investigate the dynamics associated with the interaction of tidal currents and bathymetry. The higher-resolution (6 hourly and ~12.5 km) winds from ECMWF reanalysis datasets are also used to relate the HFR currents with wind-driven currents (Dee et al., 2011; Mandal et al., 2018c).

3.2. Methodology

Firstly, to test the reliability of the HFR-derived currents, the amplitudes of the tidal constituents derived from the zonal (u) and meridional (v) currents (from HFRs) at the locations E (72.64 ºE, 20.85 ºN) and W (71.77 ºE, 20.86 ºN) were compared against the amplitudes of the tidal constituents derived from sea level datasets (from tide gauges) at Daman and Jaffrabad respectively following Mandal et al. (2018b). Further, the location W with the highest data density was chosen to derive the basic statistics by means of box plots, skewness, and frequency distribution curves along the western side. To understand the diurnal surface current variability during high and low tides along the Gulf, two additional locations along northern (N; 72.29 ºE, 21.13 ºN) and southern (S; 72.23 ºE, 20.32 ºN) sides were chosen. The circulation patterns associated with the flood and ebb currents were thereby analyzed. Moreover, tidal analysis was performed at both the spatial and temporal scales to investigate and quantify the tidally

driven currents using the T_Tide toolbox (Pawlowicz et al., 2002, source: http://www.eos.ubc.ca/~rich/t_tide/t_tide_v1.3.zip) and thereby to explore the coastal hydrodynamics. Note that for the spatial variability, the analysis has been performed only at those HFR grids having more than 75% data (Fig. 1). Moreover, while the data gaps for a few hours in some of the days do exist, but the gaps are not continuous. The reliability of the T_Tide toolbox was extensively verified by introducing such arbitrary short gaps in the continuous time-series (figure not shown). The results corresponding to analysis with short gappy time-series and without those gaps were effectively the same. Additionally, the factors (bathymetry, stratification, etc.) influencing the variations in tidal currents are also investigated.

The present study is the first of its kind in the northern Indian Ocean to characterize the asymmetry of the GoKh using both the harmonic analysis approach (as detailed in Section 5.1 later) and the skewness-based approach (see Section 5.2 later). Typically, the skewness (γ) is a quantitative measure of asymmetry as defined by (Nidzieko, 2010; Song et al., 2011; Gong et al., 2016):

$$\gamma = \frac{\mu_3}{{\mu_2}^{3/2}} \tag{1a}$$

where, the *m*-th moment about zero is defined as,

$$\mu_m = \frac{1}{N-1}\sum_{i=1}^{N}(x_i)^m \tag{1b}$$

If current velocity is denoted by '*x*', then the skewness quantifies the tidal asymmetry as a result of tidal currents. The Gulf would be flood asymmetric, if $\gamma > 0$, and would be ebb-dominant, if $\gamma < 0$. The present study is mainly focused on FVA, which is vital to understand the processes of sediment transport and erosion. The skewness-based method is applicable to any number of combinations of the tidal constituents, so, all of the significant constituents (i.e., with Signal-to-Noise Ratio > 2) are considered in this study. The dominant and significant major (shallow water) tidal constituents in this domain are M2, S2, K1, and O1 (M4 and MS4). However, note that the SNR was slightly above unity for S2 in the north and MS4 in the east; while in the north, the SNR for K1 and MS4 was slightly less than 2 (see Table 1). Based on the results from the quantification of dominating tidal constituents extracted from the HFR currents in the GoKh (see Section 4.2.2 later), and earlier studies from Nayak

and Shetye (2003) and Unnikrishnan et al. (1999a), three combinations (based on the combination of Doodson frequencies, $\omega_1 + \omega_2 = \omega_3,\ 2\omega_1 = \omega_2$) are considered in the present study; the interaction between K1, O1 and M2 (γ_0), the interaction between M2, S2 and MS4 (γ_1) and the interaction between M2 and M4 (γ_2) (Song et al., 2011). These combinations are considered in this study as the GoKh has mixed, mainly semi-diurnal tidal regime (F-ratio between 0 and 1.5). The asymmetry induced by the interaction of all these combinations (Gong et al., 2016; Song et al., 2011) is,

$$\gamma_0 = \frac{\frac{3}{2}\, a_{D1}^2\, a_{D2} \cos(2\varphi_{D1} - \varphi_{D2})}{\left(a_0^2 + \frac{1}{2}\sum_{i=1}^{N} a_i^2\right)^{3/2}} \tag{2}$$

$$\gamma_1 = \frac{\frac{3}{2}\, a_{D2}'^2\, a'_{D4} \cos(2\varphi'_{D2} - \varphi'_{D4})}{\left(a_0^2 + \frac{1}{2}\sum_{i=1}^{N} a_i^2\omega_i^2\right)^{3/2}} \tag{3}$$

$$\gamma_2 = \frac{\frac{3}{4}\, a_{M2}^2\, a_{M4} \cos(2\varphi_{M2} - \varphi_{M4})}{\left(a_0^2 + \frac{1}{2}\sum_{i=1}^{N} a_i^2\omega_i^2\right)^{3/2}} \tag{4}$$

$$\gamma_3 = \frac{\sum_{i=1}^{N} \frac{3}{2}\, a_i^2\, a_0 \cos(\varphi_0) + a_0^3 \cos(\varphi_0)}{\left(a_0^2 + \frac{1}{2}\sum_{i=1}^{N} a_i^2\right)^{3/2}} \tag{5}$$

$$\gamma_0 + \gamma_1 + \gamma_2 + \gamma_3 = \gamma_{total} \tag{6}$$

where, a_i and φ_i (a_0 and φ_0) are the amplitudes and phases of tidal constituents (residual component), respectively. *D1 (D2')* is the combination of K1 and O1 (M2 and S2) in Equation 2 (3), whereas *D2 (D4)* represents M2 (MS4). γ_3 is the contribution from the residual current flow. The derivation of all these components is explained in detail in Gong et al. (2016) (see their Section 3.3 and Appendix). A positive (negative) residual flow has a phase value of 0º (180º) (Gong et al., 2016). In the present study, φ_0= 180º, N = 6, the residuals are mostly negative during the period of study. γ_{total} is the total asymmetry by all the combinations.

4. Results and Discussions

In this section, the HFR currents are first analyzed to explain the diurnal variability (in a day) of surface circulation patterns (Subsection 4.1), followed by the tidal analysis of the HFR surface currents with a special focus on the shallow-water tidal constituents in Section 4.2. The hourly HFR currents are also statistically analyzed to provide detailed statistical metrics, which are discussed in Appendix B.

The statistical metrics indicate that the HFR could detect and quantify the tidal variability (Appendix B) reasonably well in agreement with past studies (Unnikrishnan et al., 1999b). Generally, the main driving forces of ocean surface currents are wind forcing and density-driven currents in the open ocean, whereas, near the coastline, it is driven both by the tides and local winds (Port et al., 2011). However, earlier studies have reported that the currents in the entire Gulf are driven by tides alone (Nayak and Shetye, 2003; Nayak et al., 2015). This provided the motivation to discuss the tidal variability of HFR surface currents and factors contributing to the amplification of tides in Section 4.2.

4.1. Diurnal Circulation Variability of HFR Surface Currents

The spatial variation of the current pattern was subject to study due to the lack of observations. In this section, the diurnal circulation variability is quantified at four locations – S, E, N, and W, based on continuous data availability for 24 hours (09:00 hrs, 26 May 2012 – 08:00 hrs, 27 May 2012). The evolution of surface currents during a typical spring tide semi-diurnal cycle is observed to propagate in the order: S – E – N – W and then towards the open sea (Fig. 3). The anti-clockwise circulation pattern dominates the flow, which is comparable to the current propagation in the GoKh, representing how the current changes with the propagation of tides in the GoKh.

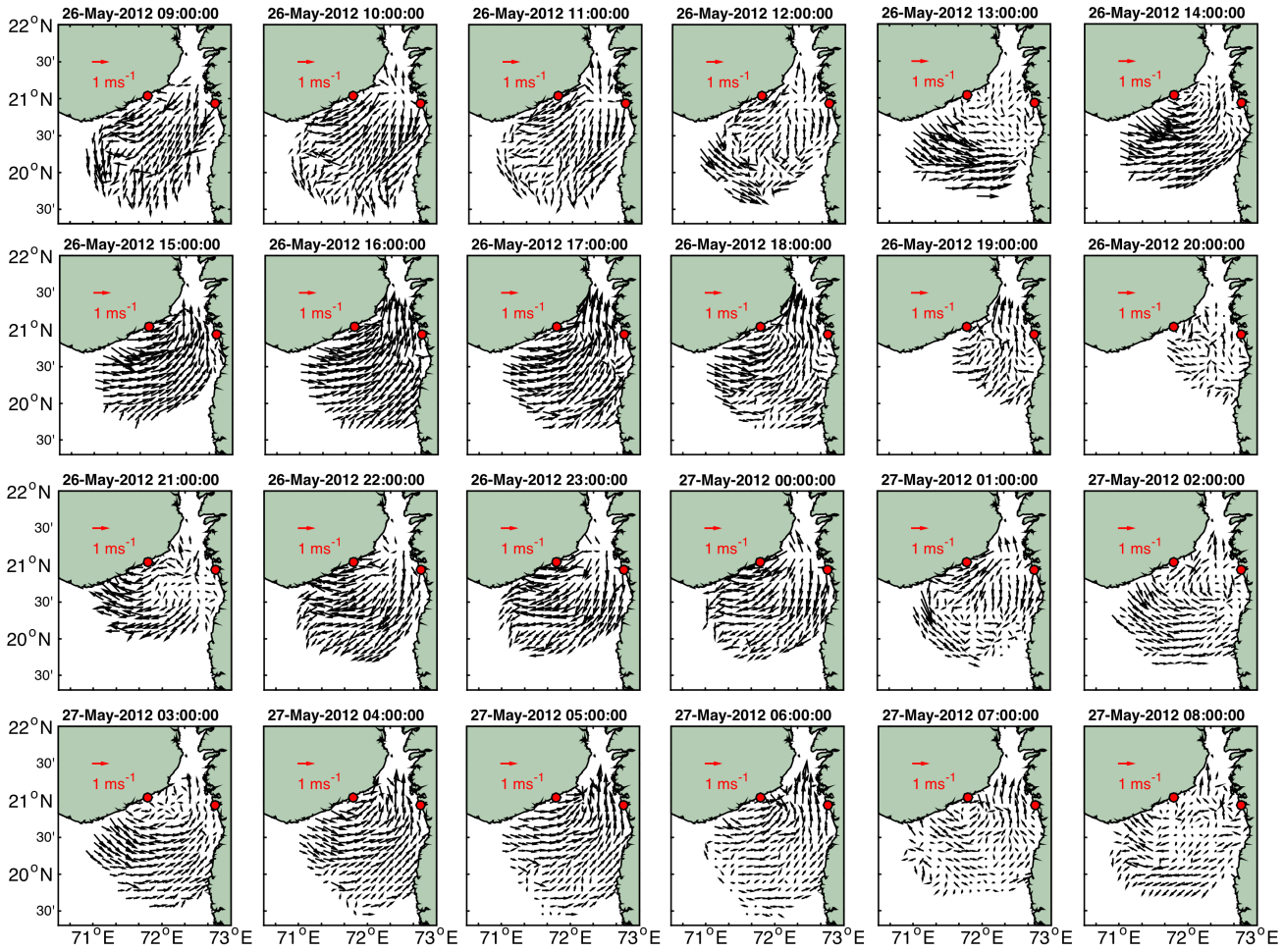

Fig. 3: Diurnal spatial variability of HFR surface currents from 26th May 2012 (09:00 hours) to 27th May 2012 (08:00 hrs). Red dots indicate HFR stations at Wasi and Jegri, Gujarat, India.

Besides, it is evident that the location W (N and E), along the western (northern and eastern) part of the GoKh, experienced the highest ebb (flood) currents with peak current speed of ~1.08 (2.00 and 1.22) m s^{-1} during 22:00 hrs, 26 May– 00:00 hrs, 27 May (16:00 hrs, 26 May – 18:00 hrs, 26 May) (Figs. 4b-4d). However, on the southern part of Gulf (at location S), the currents (~1.20 m s^{-1}) are symmetric in nature and reverses twice in a day (Fig. 4a), indicating a semi-diurnal tidal cycle (generally characterized by two simultaneous cycles of high and low tide).

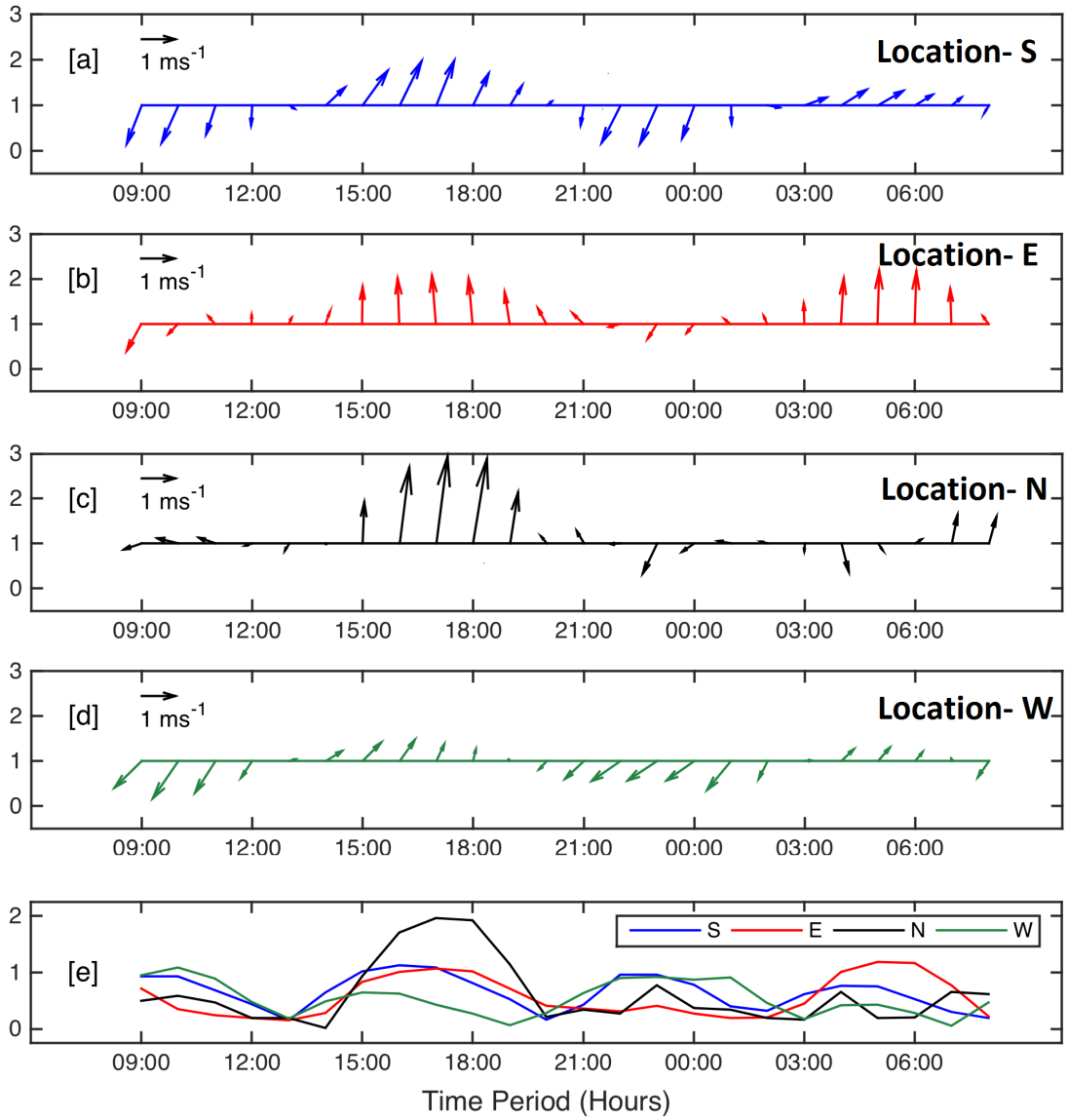

Fig. 4: The current direction showing diurnal variability of HFR currents at location (a) S (blue), (b) E (red), (c) N (black), and (d) W (green), with locations shown in figure 1. The current magnitude (cm s^{-1}) comparison at all locations is shown in (e) during 09:00 hrs 26 May-08:00 hrs 27 May 2012.

During a flood (ebb) current, when water level rises (falls) between low and high tides, currents flow towards (away from) the Gulf. However, the strongest currents occur midway between the high and low tides (Unnikrishnan et al., 1999a). It is interesting to note that along the northern and eastern parts, the flood currents are stronger and stay longer in comparison to ebb currents, which are weaker and stay for shorter periods. This is due to the non-linear friction-induced damping in the shallow waters, which influences the propagation of water level changes (Jena et al., 2018; Manoj et al., 2009). Moreover, slack tides are also observed during the reversal of currents (Fig. 4e). The change of direction of currents near high and low tides (transition period) leads to the generation of slack tides. So, this movement of huge

water quantities generates the strongest tidal currents with changes in tides (high to low or vice-versa). Also, during the movement of waters between the head and mouth of the Gulf, the tidal currents lead a parallel flow (Pugh and Woodsworth, 2014).

4.2. Tidal Analysis of HFR Surface Currents

This section focuses on the validation of the HFR-derived surface current constituents against those available from tide gauge observations, and the harmonic analysis of currents to extract the higher-order tidal constituents. Therefore, tidal analysis has been performed individually at all the locations – E, W, N, and S, and also on a spatial scale to quantify the dominant tidal constituents during high and low tides (flood and ebb currents) and to analyze the tidally driven currents along the Gulf.

4.2.1. Validation of tidal constituents

Due to the scarcity of *in situ* surface current observations in this region, a detailed harmonic analysis of the HFR surface currents (at all locations) is first presented to compare the presence of 28 tidal constituents against those obtained from independent tide gauge sea level datasets at Daman and Jaffrabad following the comparison methodology documented in Mandal et al. (2018b). The quantitative regression analysis is performed to compare the amplitudes of the corresponding tidal constituents obtained from the harmonic analysis of both parameters; currents (Figs. 5a and 5b) and sea-level heights (Figs. 5c and 5d). The circulation pattern in GoKh is dominated by the meridional currents; hence, the tidal elevation constituents are indeed well correlated with those of the meridional component of HFR currents (Figs. 5a-5d). For all the tidal constituents, the corresponding amplitudes from the HFR zonal (meridional) currents are higher along the western (eastern) sides of the Gulf. For the major (M2, S2, N2, K1, O1) tidal constituents, the correlation coefficients are 0.99 and 0.97 (0.75 and 0.77) at Daman (Jaffrabad), respectively for u and v components. Similarly, for the minor (SK3, M4, MS4, M6, M8, etc.) tidal constituents, the corresponding correlation coefficients are 0.73 and 0.90 (0.76 and 0.96) at Daman (Jaffrabad) for u and v components, respectively.

These comparisons indicate that the low-frequency tidal constituents (diurnal and semi-diurnal) extracted from the HFR currents match relatively well with the sea level variations than the ones with higher frequencies. However, the fact that higher tidal current amplitudes from zonal (meridional) currents at location W (E) implies that the current pattern is dominated by zonal (meridional) currents along the western (eastern) regions of the GoKh. The higher significance of all the tidal constituents is

quite evident for resolving both the major and shallow-water constituents from the HFR currents in the Gulf. These results highlight the possibility of utilizing the HFR datasets for understanding near-coastal processes.

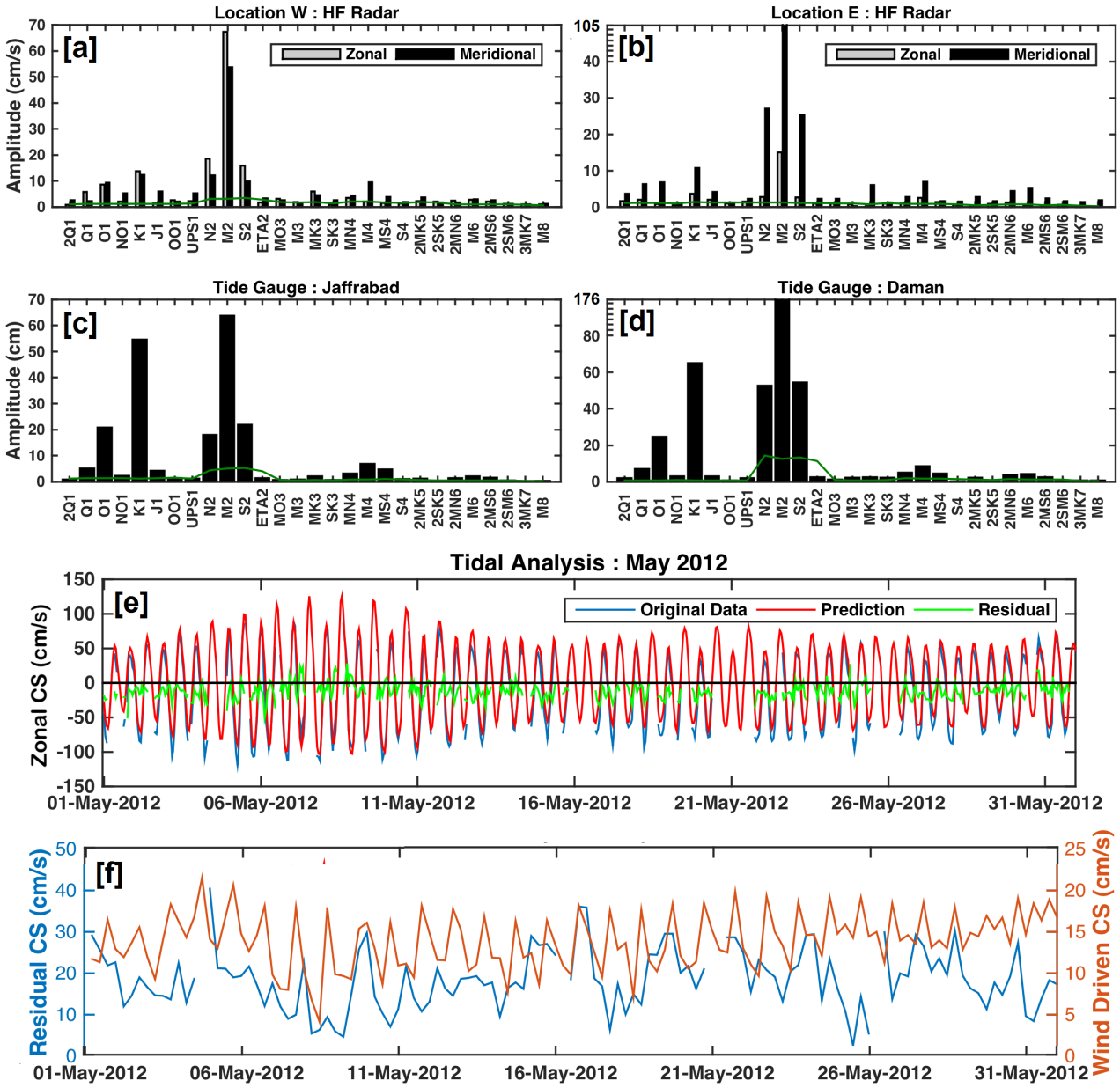

Fig. 5: The magnitude of tidally driven currents (in cm s^{-1}) for zonal (grey) and meridional (black) components of the HFR current data at the locations (a) W and (b) E are indicated in bars. Similarly, for the tidal heights from tide gauges are shown at the locations (c) Jaffrabad and (d) Daman. The x-ticks indicate the tidal constituents. The amplitude errors are indicated by the dark green line. (e) The hourly variability of the zonal component of HFR data before and after tidal analysis. The blue, red, and green lines correspond to original, predicted, and residual data, respectively. (f) The 6-hourly variability of wind-driven currents and residual currents at location W.

4.2.2. Semi-diurnal tidal current variability (M2 and S2)

The tidal harmonic analysis along the western GoKh at location W using HFR-derived currents (zonal component shown in Fig. 5e) indicates the presence of two spring and neap tides, which compares well with results in Fig. B.1a (see Appendix B). Tidal predictions are generally based on the proposition that the ocean surface currents variability can be estimated by the superposition of constant current amplitudes and phases corresponding to the harmonics. The residual currents corresponding to the detided data, varying in the range 2-45 cm s^{-1}, indicate the non-occurrence of any extreme events during the period of analysis (Figs. 5e and 5f). The poor match (correlation coefficient: 0.15) between the residual currents and wind-driven currents from the higher-resolution ECMWF winds near the same location shows that winds contribute very little to drive the currents in the Gulf (Fig. 5f). However, a strong peak at 24 hours is observed from the wind-driven current spectra, but with much lesser amplitude (~10% of K1 tide) in comparison to the total tidal currents (figure not shown).

Table 1: Ellipse characteristics from harmonic tidal analysis of currents (u+iv) at W (-10 m), E (-30 m), S (-100 m), and N (-15 m). The depths are given in brackets.

Tidal Constituents	Time Period (hrs)	Major Axis (cm s^{-1})				Minor Axis (cm s^{-1})				Signal to Noise Ratio (SNR)			
		W	E	N	S	W	E	N	S	W	E	N	S
O1	25.82	11.73	6.85	27.22	11.70	4.72	-0.76	-1.13	0.75	21	4.8	2.6	13
K1	23.93	16.24	10.90	10.90	15.43	9.03	-3.27	-6.92	2.86	43	12	1.8	21
N2	12.66	22.00	27.17	35.23	21.21	1.97	0.31	1.40	1.29	24	32	7.4	55
M2	12.42	86.05	105.86	30.26	80.43	2.30	6.54	12.04	11.07	420	480	6.3	640
S2	12.00	18.36	25.43	12.92	21.34	3.18	1.54	-3.38	-1.03	20	22	1.1	51
M4	6.21	9.64	7.47	29.99	2.61	1.32	-0.54	-0.77	-0.97	13	15	31.0	2
MS4	6.10	4.08	1.76	6.55	2.87	0.57	1.28	0.88	0.42	2.5	1.1	1.9	2.8
Percent total variance predicted/ variance original for locations W, E, N, and S are 91.8, 94.3, 50.5, and 90.1 %, respectively. Negative minor axis means clock-wise circulation.													

The harmonic analysis at location W (with highest data availability) indicates that the M2 tidal constituent has maximum amplitudes of 67.32 cm s^{-1} and 53.65 cm s^{-1} for the zonal and meridional currents, respectively (Fig. 5a), which dominates among all other tidal constituents. The other leading significant tidal constituents with higher amplitudes are N2 (18.49, 12.10 cm s^{-1}), S2 (15.85, 9.80 cm s^{-1}) and K1 (13.82, 12.43 cm s^{-1}), followed by O1 (8.61, 9.26 cm s^{-1}), respectively for u and v components

(Fig. 5a). The order of tidal constituents (in terms of amplitudes) obtained from the HFR currents compares well with those obtained from the tide gauges (Figs. 5a and 5c). Similar results are obtained at location E (Figs. 5b and 5d), but with higher amplification of tidal constituents derived from the meridional component, than at location W. Moreover, the HFR datasets clearly indicate that the predominant semi-diurnal tidal constituent, M2, is about 4.5 times stronger than the major diurnal constituent, K1. Here, the total tidal variance corresponding to the v-component (95.7%) is higher than that of the u-component (86.3%). Tides have also been characterized in terms of form number ratio (F-ratio) of tides (Murty and Henry, 1983). The highest (lowest) value of F-ratio is found to be ~1.12 (0.26) near the head (mouth) of the Gulf, which indicates that the tidal regime is of mixed, predominantly semi-diurnal type. The results corresponding to harmonic analyses at all other locations have been tabulated in Table 1, indicating the dominance of M2 and S2 tides. Since these tides are significant with highest amplitudes (the semi-major axes) along the Indian coast (Jithin et al., 2017; Subeesh et al., 2013), the spatial distribution of M2 and S2 tidal ellipses in the GoKh, have been analyzed during the pre-southwest monsoon (May 2012).

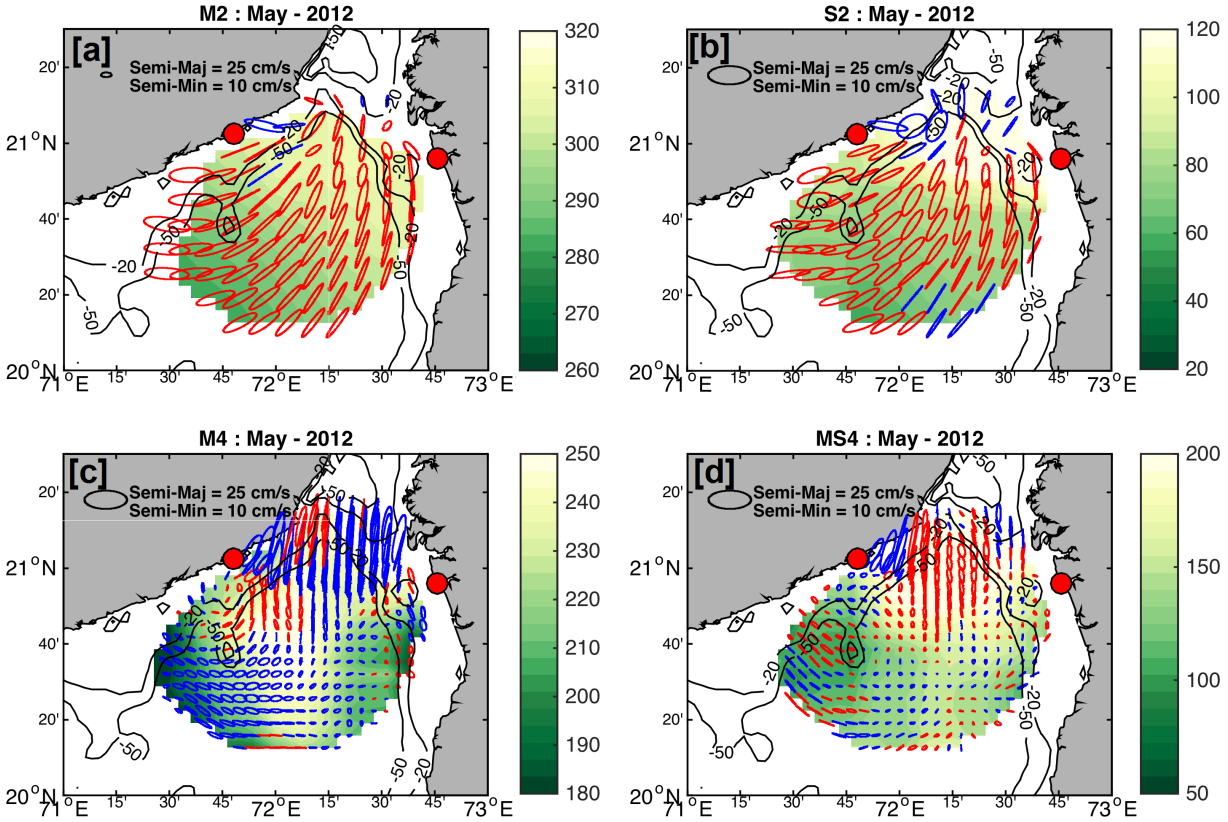

Fig. 6: (a) M2 (b) S2 (c) M4 and (d) MS4 tidal ellipses derived from harmonic analysis of HFR current data with tidal phases (shaded, in GMT). The blue (red) ellipses indicate clockwise (anti-clockwise) rotation. The black contours indicate the isobaths. Black ellipse is the reference ellipse. Red dots indicate HFR stations at Jegri and Wasi, Gujarat, India.

During the early southwest monsoon (May), the M2 tidal ellipses are observed with significant amplitudes with anti-clockwise orientation, which dominates throughout the region (comparable to anti-clockwise circulation in Fig. 3). However, a small region near the Jegri lighthouse is dominated by the clockwise ellipses (Fig. 6a). Similarly, the S2-driven ellipses are oriented anti-clockwise, but with comparatively lesser amplitudes of the semi-major axes (Fig. 6b). However, in comparison to the coverage of M2 ellipses, higher concentrations of S2 clockwise ellipses are observed all over the head region. It is to be noted that the ellipses are rectilinear and oriented quasi-parallel to 20–50 m isobaths. The orientations of ellipses remain unchanged from the continental shelf to slope throughout the region, indicating stronger tidal driven currents.

The shaded background in Fig. 6 indicates the spatial variations of tidal phases (co-tidal lines), all expressed with respect to Greenwich Meridian Time (GMT). The distribution of co-tidal lines (both M2 and S2) increases northward from the mouth to head regions of GoKh, which compare well with the earlier results from barotropic models (Testut and Unnikrishnan, 2016; Unnikrishnan et al., 1999a). The tidal phase values vary in the range 280º-320º for the M2 component, whereas the same is comparatively less for S2 (60º-120º).

Since the tidally driven currents are very strong in the entire region, a three-trajectory tidal analysis throughout the domain has been carried out from (a) S to W, (b) S to N, and (c) S to E (see Fig. 1 for the locations). Significant amplification of amplitudes corresponding to M2 tides is observed in all cases (Fig. 7, left column), with the highest being along the track from the mouth to the head of the Gulf. The amplification also continues from the mouth to the west coast (80.43 – 86.67 cm s^{-1}) and east coast (80.43 – 102.75 cm s^{-1}) of the GoKh. However, as the currents propagate from mouth to head over the continental slope, the M2 tide intensifies slowly (80.43 – 90.94 cm s^{-1}) until the shelf break. It undergoes the highest intensification (~105 cm s^{-1}) along the continental shelf but reduces further towards the Gulf head (62.15 – 30.26 cm s^{-1}) (Fig. 7, left column). Another important feature to be noted is that the individual harmonic analysis of both u- and v- components of current at the same four locations indicates an increase in the amplitude of the M2 tidal constituent for zonal (meridional) component as currents propagate from S to W (S to E, N) (figure not shown). This indicates that the current pattern is dominated

by the meridional (zonal) component along the coastline near the Wasi Borsi (Jegri) lighthouse, which confirms the earlier results in Section 4.1 (Fig. 4). The percentage total tidal variance ranged between 40 and 95% throughout the entire domain, of which the mouth of GoKh (southern region) is dominated by M2 tides with higher variance (70 – 90%) than the head region (10 – 40%). Moreover, the M4 tides contribute up to 40% of the total tidal variance at the head region. The remaining ~10% of the total tidal variance is a mixed contribution of the wind-driven and geostrophic currents (Fig. 5f). The results match well with earlier studies in other regions, which specify that the dominant tidal constituents can account for nearly 60 – 90% of the tide-induced variability (Cosoli et al., 2013; Godin, 1983; Gough et al., 2010; Noble et al., 1987). Hence, it can be concluded that the entire circulation variability in the Gulf is dominated by the tidal currents (especially the M2 tides) (Fig. 6a).

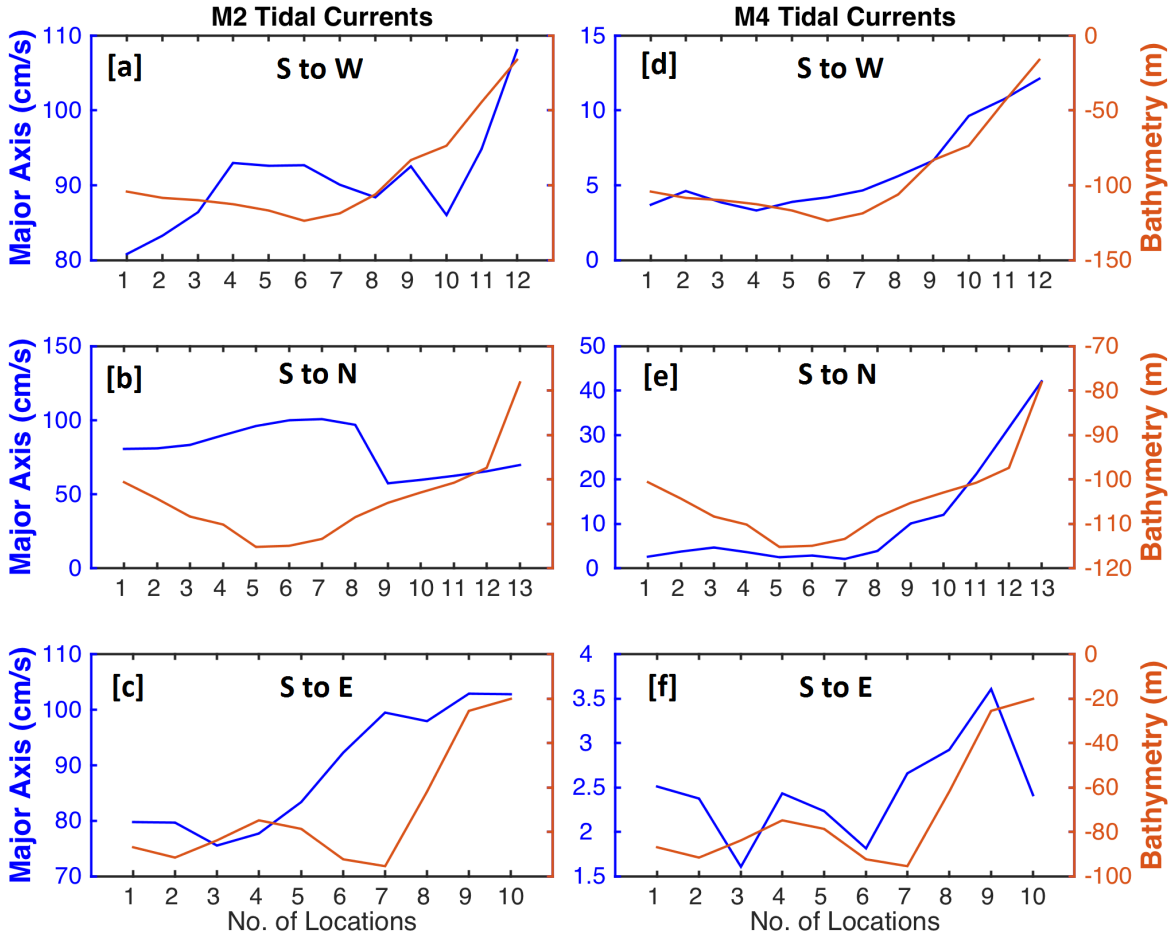

Fig. 7: The variation of semi-major axes corresponding to M2 (left column) and M4 (right column) tidal constituent with respect to bathymetry from S to N (top row), S to W (middle row) and S to E (bottom row). The numbers along the x-axis indicate the number of locations along the track.

This strong amplification of the M2-dominated semi-diurnal tides is an important characteristic of the Gulf. Generally, the possible reasons for semi-diurnal tidal amplification in every coastal area/ Gulf are the interaction with bathymetry (bottom friction), stratification, and channel geometry (Gough et al., 2010; Subeesh and Unnikrishnan, 2016). The GoKh is one of the converging channels with a decrease in cross-sectional area along the meridional direction, which indicates that the amplification (damping) of incident (reflected) waves can be attributed to the converging channel geometry and favorable resonance effects (Friedrichs and Aubrey, 1994; Nayak and Shetye, 2003). The sea surface winds and residual currents in this region do not indicate the presence of any strong relationship between the two parameters (Fig. 5f). Further, stratification is an important factor, which plays a significant role in the generation and amplification of internal tides (baroclinic effect). Weak stratification and less stability of the water column during May diminishes the effect of internal tides (Fig. 2c). Thus, the barotropic effect dominates over the baroclinic effect throughout the Gulf, as was reported by Giardino et al. (2014) and Unnikrishnan et al. (1999a). Hence, the dominance and amplification of M2 tides in the Gulf are attributed to the interaction with shoaling bathymetry and the effects of convergent channel geometry.

4.2.3. Shallow-water tidal current variability (M4 and MS4)

The HFR currents also enable the identification of the shallow water tidal constituents (MK3, M4, MS4, M6, and M8) with significant amplitudes (> 10 cm s^{-1}). The variability of M4 and MS4 tidal driven currents is observed in small patches of clockwise and anti-clockwise ellipses (Figs. 6c and 6d). In comparison to the semi-diurnal ellipses, the pattern corresponding to M4 and MS4 are dominated mostly by clockwise and anti-clockwise ellipses (Fig. 6d). It should be noted that the M4 and MS4 tidal ellipses follow the same pattern as M2 and S2 tides near the mouth of the GoKh. A sudden intensification of both M4 and MS4 tide is observed towards the head with the highest amplification for the M4 tidal ellipses (Fig. 6c). The amplitude, as well as the phase of both M4 (first harmonic of M2) and MS4 (quarter-diurnal compound resulting from M2 and S2 interactions), increases inside the Gulf.

The three-trajectory tidal analysis that has been carried out in the domain indicates the amplification of M4 tides, with the highest amplification rate along the track from the mouth to the head of the Gulf (S to N). The amplification of M4 tide continues from the mouth to the west coast (2.61 – 9.63 cm s^{-1}) and east coast (2.61 – 7.47 cm s^{-1}) of the GoKh (Table 1). However, as the currents propagate from mouth to head over the continental slope, M4 tides intensify slowly (2.61 – 4.93 cm s^{-1}) until the shelf break (Table 1). They undergo the highest intensification at the Gulf head (4.94 – 29.99 cm s^{-1})

(Fig. 6c). At location N, the amplitudes corresponding to M4 (29.99 cm s^{-1}) and M2 (30.26 cm s^{-1}) tides are comparable (Fig. 6c). This sudden intensification can be attributed to the bathymetry interaction and funnel-shaped structure of the Gulf (Fig. 7, right column). The lower frictional influence on the narrow continental shelves can lead to the anti-clockwise orientation of ellipses along with the bathymetry (Battisti and Clarke, 1982). This is the most influential factor for different orientations of M4 and MS4 ellipses. However, other factors may also be involved with lesser contributions to this phenomenon. So, further analysis is needed via three-dimensional coastal hydrodynamic modeling to investigate the mechanisms of tidally driven currents on an inter-seasonal scale.

5. Tidal Asymmetry in the Gulf of Khambhat

The spatial variation of F-ratio (0-1.5) indicates that the GoKh has mixed, predominantly semi-diurnal tidal regime (figure not shown). The nature of tidal asymmetry has been investigated distinctly using the two aforementioned methods; (i) the harmonic analysis method (Section 5.1), and (ii) the skewness-based approach (Section 5.2), in which the asymmetry is quantified using skewness parameter at first, followed by the quantification of individual contributions from the three combinations -- K1/O1/M2, M2/S2/MS4 and M2/M4, and the residual flow.

5.1. Harmonic Analysis Method

In the domains with the mixed, mainly semi-diurnal tidal regime and strong tidal flats, tidal asymmetry generally arises due to the interaction of principal tides (M2) with higher harmonics (M4), as generated by distortions (Speer and Aubrey, 1985). The spatial variability of tidal current asymmetry from both u- and v-components are investigated using the amplitude ratio and relative phase (Fig. 8).

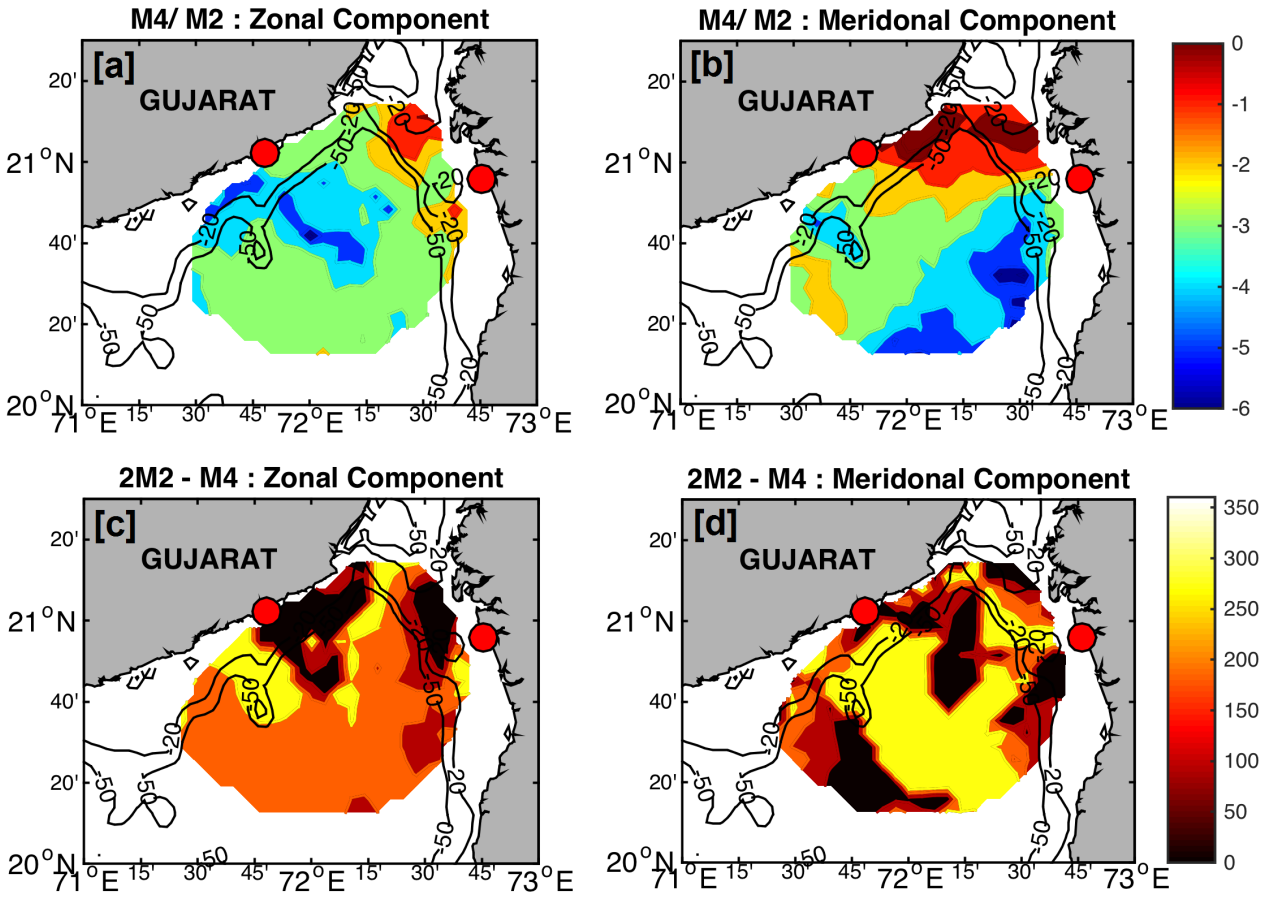

Fig. 8: The M4/M2 amplitude ratio (in log scale) for the (a) zonal and (b) meridional components. The 2M2 – M4 relative surface phase for the (c) zonal (d) meridional components of HFR surface currents. The black contours indicate the isobaths (-20 and -50 m).

The tidal amplitudes corresponding to semi-diurnal (M2, S2, and N2) and diurnal (K1 and O1) tidal constituents increase towards the head regions of the Gulf. Also, the tidal analysis shows the amplification of the M4 tidal constituent (Fig. 6c) along with the non-linear amplification of compound tides (MK3, MS4, MN4, and others) (Figs. 5a and 5c). The intensification of M4/M2 amplitude ratio is observed towards the mouth as well as along the eastern and western coasts of the Gulf (Figs. 8a and 8b), showing that the tides do not get distorted much offshore (area near S), whereas, inside the Gulf, tides undergo complete distortion (as evident from the high amplitude ratio, 0.5). In addition, current asymmetry is more evident towards the mouth from the meridional currents, whereas zonal currents are more distorted along the eastern GoKh (Figs. 8a and 8b). The higher degrees of tidal asymmetry at the head of the Gulf can be attributed to the shallow bathymetric features of this region (Fig. 8b).

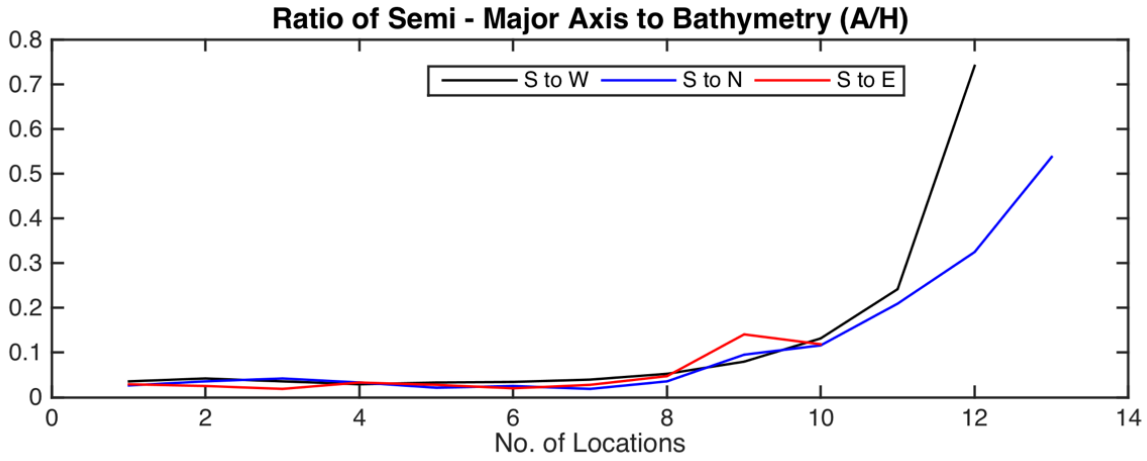

Fig. 9: Variations in the ratio of the semi-major axis and bathymetry (Amp/H) along three trajectories from S to W, N, and E as indicated in figure 1.

According to Friedrichs and Aubrey (1988), the surface relative phase relationship between M2 and M4 is as follows: a flood-dominant system has a phase of 90º to 270º with maximum flood currents at 0º/360º, and an ebb-dominant system has a phase of 90º to 270º with maximum ebb currents at 180º (Fig. 2 of Friedrichs and Aubrey, 1988). The eastern and western GoKh regions are mainly dominated by flood asymmetry in the case of zonal currents, while the offshore region (near S) is mainly dominated by ebb asymmetry (Fig. 8c). Similarly, the whole domain is flood-asymmetric, as observed from meridional currents (Fig. 8d), except for some small mudflat regions that can increase the ebb dominance. Since the meridional currents dominate the whole Gulf, the GoKh can be characterized as a flood-asymmetric region, although offshore regions experience less tidal distortions. Flood dominance characteristics are associated with the non-linear tidal distortions in the shallow bathymetry, which is represented by the ratio of the semi-major axis to bathymetry (A/H) (Friedrichs and Aubrey, 1988). This ratio for the GoKh is presented in Fig. 9 for the three pathways from the open southern side of the Gulf (S) to the northern (N), eastern (E), and western (W) regions of the Gulf. This ratio indeed increases with the propagation of tides inside the Gulf (Fig. 9), confirming the existence of the non-linear tidal distortions in the presence of shallow and complex bathymetry of the GoKh.

5.2. Skewness-Based Approach

Nidzeiko (2010) has proposed a methodology to quantify tidal asymmetry in the estuaries of California. The tidal asymmetry factor (β) is defined by $\beta = a\,(1+\alpha)\,h\, -(\bar{b}\, - B)/\,\bar{b}$ (Nidzieko, 2010), where, a is half of the tidal range, α = 0.5 is the weighting coefficient (Nidzieko, 2010), h is mean depth, L, b and B are the length, total width and main channel width of the estuary, respectively and $\bar{b} =$

$(b + B)/2$. This tidal asymmetric factor, β was parameterized to estimate the relative importance of depth and width of the estuary over a tidal cycle (Friedrichs and Madsen, 1992). The domain would be flood-asymmetric if $\beta > 0$, and would be ebb-asymmetric if $\beta < 0$. In this study, the same methodology has been applied to the GoKh, considering the Gulf to be an equivalent estuary in its present topographic configuration. The Gulf is about 200 km long (L) and about 125 km wide (b), with a narrow main channel of about 60 km (B). Since the tidal range (a) and the depth (h) vary considerably from the west (near Jaffrabad) to the east (near Daman), a range of values for these parameters are chosen to compute the morphological asymmetry. The value of *'a'* is 1.5 (3.8) m at Jaffrabad (Daman). The mean depth of the channel (h) near the location of the tide gauge at Jaffrabad (Daman) is ~4 (9) m. The range of computed asymmetry factor (β = 0.21 and 0.28 along the western and eastern GoKh, respectively) indicates that the domain is flood asymmetric.

Furthermore, this asymmetry is quantified by skewness (γ) and third moment (μ_3) from the HFR-derived surface currents covering most of the Gulf and along four different transects (Fig. 10). The skewness-based approach was discussed in detail in methodology (Section 3.2). The spatial distribution of skewness (Fig. 10a) follows the pattern of the direction of the flow of tidal currents in the Gulf (Fig. 3). Most of the Gulf is flood-asymmetric with positive skewness and third moment, while two small regions near the mouth of the Gulf at the two ends (southeast and southwest) is found to be ebb-asymmetric with negative values of both skewness and third moment (Figs. 10a and 10b). Zero contours of skewness and third moment indicate the region where the tidal currents are symmetric and signify the change-over from flood-dominance to ebb-dominance. Higher values of positive skewness (>0.20) and third moment (>0.04) over the head regions of the Gulf indicate higher non-linear distortions during the rise and fall of the water levels here in comparison to the open ocean.

Four transects have been chosen in the domain to further focus on the along-track variability (Figs. 10a and 10b). The variations of both the statistical measures along the tracks 1 and 2 show positive values throughout the Gulf, with the highest values along the head of the Gulf (main channel) indicating flood dominance (Figs. 10c and 10d). Moreover, two peaks are observed in the variations of the third moment along both the tracks. The first peak (in the offshore regions) is due to a higher standard deviation of M2 tidal currents, whereas the second peak (near head Gulf) is due to the M4 tidal currents. Similarly, the same parameters are quantified along the tracks 3 and 4 for the meridional currents (Figs. 10e and 10f). The variations along track 3 are comparatively higher than track 4, with highest values of skewness and third moment at the mid-Gulf. Higher values of both the parameters in the mid-Gulf (near coast

regions) are attributed to the higher standard deviation of M2 (M4) tidal currents. The positive values of both the skewness and third moment along all transects account for the flood asymmetry in the GoKh.

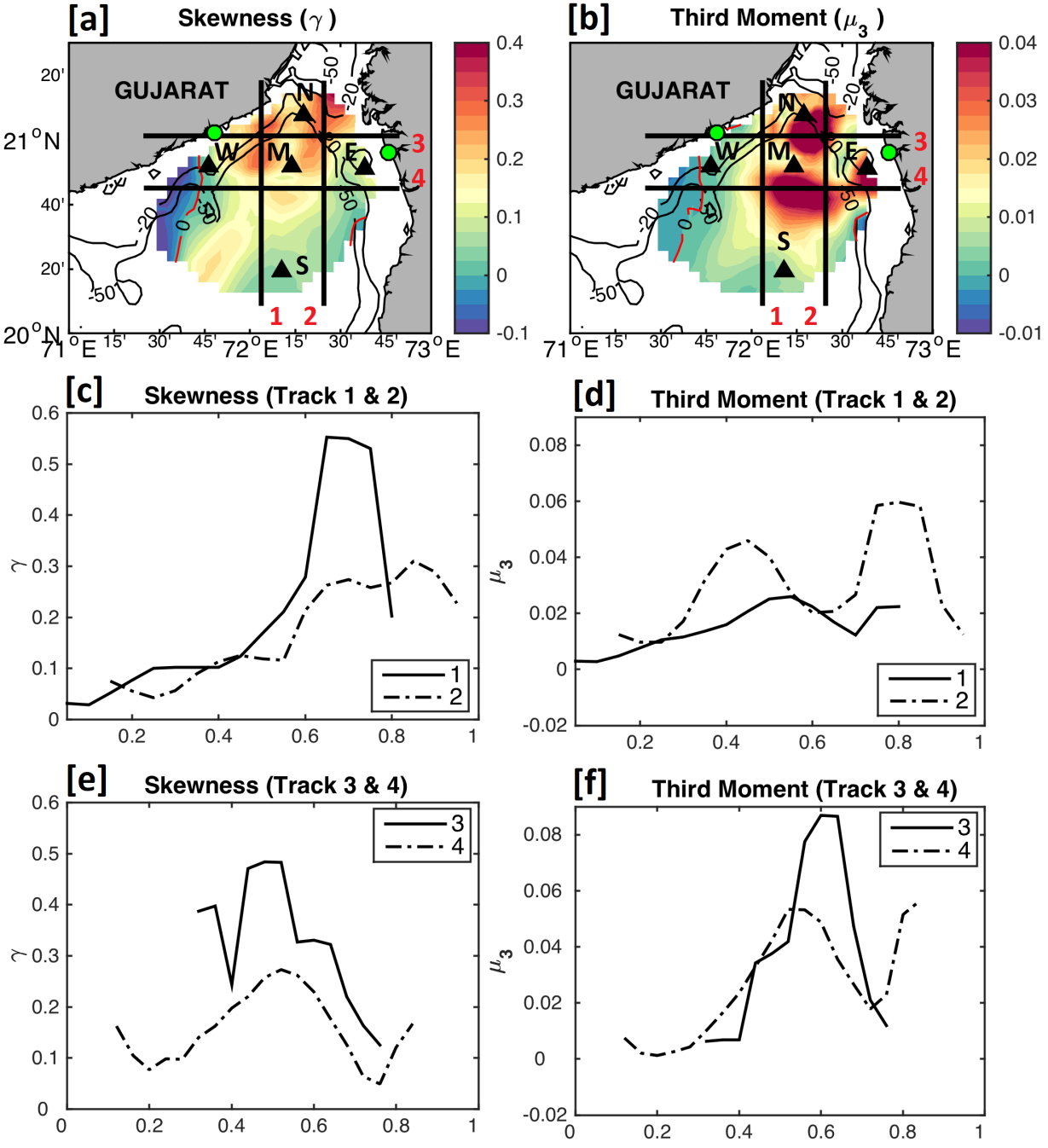

Fig. 10: The spatial variability of (a) skewness and (b) third moment is in color overlaid on bathymetry (black contours). The zero contours of skewness and third moment (red line) signify the change-over from flood-dominance to ebb-dominance. The along-track variability of skewness and third moment about the mean currents are shown against the normalized distance in the x-direction along tracks 1 and 2 (c and d), and tracks 3 and 4 (e and f). Tracks are shown in thick black lines in (a) and (b).

The individual contributions from the different combinations of tidal constituents towards asymmetry (described in Section 3.2, Eqs. 2-5) are quantified in Table 2. The FVA induced by the interaction of M2 and M4 (overtides) exhibits distinct variations in the Gulf. This contribution (γ_2) is dominant at both western (0.207) and eastern (0.072) Gulf while being significant (0.045) in the mid-Gulf region along the latitudinal transect. This difference is due to the interaction of tidal currents with complex bathymetry and strong tidal flats in the domain. Moreover, the amplitude of this combination showed a reasonable increase from the southern part (S, 0.040) to middle Gulf (M, 0.045) due to the increase in the tidal current amplitudes of M2 and M4 along the longitudinal transect, whereas it decreases to the head Gulf (N, 0.012). Overall, the contribution of this overtide component favors flood dominance.

Table 2: The total asymmetry of the GoKh in terms of contributions from the different combinations at the locations shown in figure 1. $\gamma > 0$ indicates flood-dominant asymmetry.

Locations	F-Ratio	γ_{total}	K1/O1/M2 (γ_0)	M2/S2/MS4 (γ_1)	M2/M4 (γ_2)	Residual (γ_3)
E	0.17	0.079	0.003	0.005	0.072	-0.001
W	0.26	0.219	0.005	0.008	0.207	-0.001
N	0.92	0.040	0.008	0.023	0.012	-0.003
S	0.27	0.067	0.017	0.011	0.040	-0.001
M	0.29	0.243	0.088	0.111	0.045	-0.001

The asymmetry induced by the combination of diurnal and semi-diurnal constituents (K1/O1/M2) (compound tides, γ_0) is also positive throughout the region. Similar to the M2/M4 combination, the skewness of the compound tides also increases from the southern part (0.017) to the mid regions (0.088) and further decreases at the head (0.008). The initial increase is due to an increase in the tidal current amplitudes of the principal tides, followed by a decrease, which can be attributed to the difference in the phase values between diurnal and semi-diurnal tides. In contrast, the skewness is comparatively lower, but, is positive along the western and eastern regions. The contributions of the M2/S2/MS4 (γ_1) combination are also consistent with the other two and favors flood dominance. Note that γ_1 dominates the other contributions in the shallow waters in the North near the head of the Gulf. It also compares well with (γ_0) in secondary contribution to skewness in the middle of the Gulf. The contribution from the residual flow (γ_3) towards the total skewness is negligible (about 1%).

To conclude, all these combinations, along with the Gulf morphology, predominantly indicate flood dominance in the Gulf. The overtide M2/M4 combination accounts for the maximum contribution along the eastern, western, and southern parts of the Gulf, whereas the compound tides (M2/S2/MS4) have maximum contribution along with the longitudinal transect from the middle to head regions. The results from the skewness-based approach justify those from the harmonic analysis method, and thereby the GoKh can be characterized as flood asymmetric.

6. Summary and Conclusions

This study presents the first results from a comprehensive analysis of HFR-derived ocean surface currents in the GoKh, which is relatively shallow with complex bathymetry and has strong tidal flats. The high-frequency current variability and associated dynamics are investigated during May, 2012 (i) to spatially quantify the major and shallow water tidal currents; (ii) to investigate the impact of bathymetry on the amplitude variations of tidal currents in a funnel-shaped Gulf and, finally (iii) to determine the nature of tidal asymmetry in the Gulf. The major results of this study are summarized below.

- The hourly HFR currents show spring-neap variability, with the maximum current speed of ~2.0 (1.5) m s^{-1} during spring (neap) tides. Both the zonal and meridional components follow a bimodal distribution, evidently showing higher variability along the north-south direction (for the meridional component), which is due to the funnel-shaped geometry of the Gulf.

- The comparisons of HFR currents with tide gauge-derived sea-level heights at Daman and Jaffrabad, in terms of the order of the amplitudes of tidal constituents, indicate a higher correlation for the meridional component for both the major (>0.77) and minor (>0.90) tidal constituents. The highest values of 0.97 (0.96) for major (minor) tidal constituents are along the eastern (western) sides of the Gulf.

- The M2 tidal currents dominate in the Gulf, followed by other semi-diurnal (S2 and N2) and diurnal (K1, O1) tidal constituents. The M2 (86.05 cm s^{-1}) tidal currents are ~4.5 stronger than the K1 (16.24 cm s^{-1}) tidal currents. Also, the semi-diurnal tidal ellipses are anti-clockwise throughout the Gulf.

- The HFR currents enable the identification of shallow-water tidal currents (M4 and MS4) with significant amplitudes, which undergo the highest intensification at the head of the Gulf and shallow

water regions. Interestingly, the amplitudes corresponding to M4 (29.99 cm s^{-1}) and M2 (30.26 cm s^{-1}) tides are comparable at the head.

- Circulation pattern in the Gulf is predominantly driven by tidal currents, with the total tidal variance being ~90% of the total current variance. The M2 tidal currents account for 70-90% of the total tidal variance throughout the Gulf, except at the head, where about 10-40% tidal variance is from M4 tidal currents.

- Interaction with shallow bathymetry and converging channel geometry plays a significant role in the non-linear distortions and amplification of M2 and M4 tidal currents at the head of the Gulf and shallow water regions. Interestingly, the impact of stratification is found to be negligible during May 2012.

- The harmonic analysis method indicates that the head region is highly tidally asymmetric due to a higher M4/M2 amplitude ratio. The relative phase (2M2 –M4) indicates the dominance of flood currents over the head region with stronger tidal distortions.

- The asymmetry factor (β varies in the range 0.21 – 0.28) in the GoKh (dependent on Gulf morphology) evidently characterizes the Gulf as flood asymmetric. The skewness-based approach (positive values of both skewness and third moment) helped quantify this flood dominance as outlined next.

- The overtide combination (M2/M4) is the major contributor to the flood asymmetry, followed by the compound tide combination (M2/S2/MS4) in most of the Gulf. The overtide M2/M4 combination has major contributions along the eastern, western, and southern parts of the Gulf, whereas the compound tide M2/S2/MS4 combination contributes more along the longitudinal transect from the middle to the head of the Gulf.

The results from this study identify the GoKh as a promising site for tidal power generation. Also, tidal asymmetry is important to understand the development of morphology of the Gulf, via sediment transport. This study is the first to reveal the nature of tidal asymmetry utilizing surface currents in the GoKh along the Indian coast using both harmonic analysis and skewness-based approaches. The

technique developed here can be successfully applied to investigate the nature of tidal asymmetry in the nearby Gulf of Kutch and other well-known estuaries along the Indian coast (e.g., Hooghly, Mahanadi and Narmada estuaries), either using tide gauge datasets or by barotropic models. Moreover, the results presented in this study can be a significant contribution to the feasibility and implementation of the Kalpasar Project (http://kalpasar.gujarat.gov.in/mainpage.htm), which aims to build a dam and connect the two sides of the Gulf.

This study shows that during this season (May) in the Gulf, with negligible impacts of stratification and winds, the entire circulation pattern is driven by the tidal currents rather than by other forcing such as the wind-driven currents or the buoyancy currents. Investigations with the year-long datasets should be carried out to reveal the inter-seasonal variations which might be dominated by winds or buoyancy during monsoon and post-monsoon periods. Furthermore, there is also a need to fill the temporal and spatial gaps of the HFR currents using multiple new techniques such as, the Data Interpolating Empirical Orthogonal Functions (Beckers and Rixen, 2003), the Open Model Analysis (Kaplan and Lekien, 2007) and the Self Organising Maps (Kohonen, 1982, 1997), which will be part of future studies.

7. Acknowledgement

SM and SS acknowledge the Indian Institute of Technology Bhubaneswar (IITBBS) and INCOIS, Ministry of Earth Sciences (MoES) funded project (Grant No: INCOIS;F&A:O-MASCOT:2018-20:09) for financial and infrastructural support. AG acknowledges NOAA funding (NA11NOS0120038) for operational modeling. Also, SM sincerely thanks Mr. Arunraj K.S. and the entire Coastal and Environmental Engineering Group (CEE), National Institute of Ocean Technology (NIOT), Chennai for constant monitoring of the HFRs and Data Management Group of INCOIS, Hyderabad for providing the data. We sincerely thank Mr. Frank Smith of SMAST for carefully editing the revised manuscript. SM also acknowledges Ms. Panchali Bhattacharya from IITBBS for her help in formatting the manuscript. The authors highly acknowledge and thank the editor and anonymous reviewers for their comprehensive suggestions and encouraging comments. All the figures are generated in MatLab.

7. References

Antony, M.K., Shenoi, S.S.C., 1993. On the flow, thermal field and winds along the western continental shelf of India. Cont. Shelf Res. 13 (4), 425–439.

Arunraj, K.S., Jena, B. K., Suseentharan, V., Rajkumar, J., 2018. Variability in eddy distribution associated with East India Coastal Current from HF Radar Observations along South-East Coast of India, J. Geophys. Res. – Oceans, 123 (12), 9101-9118.

Aubrey, D. G., Speer, P. E., 1985. A study of non-linear tidal propagation in shallow inlet/estuarine systems. Part I: Observations. Estuar. Coast. Shelf Sci. 21 (2), 185–205.

Barrick, D. E., Evans, M.W., Weber, B. L., 1977. Ocean surface currents mapped by Radar. Sci. 198 (4313):138–144. doi:10.1126/science.198.4313.138.

Battisti, D. D., Clarke, A. J., 1982. A simple method for estimating barotropic tidal currents on the continental margins with specific application to the M2 tide off the Atlantic and Pacific coast of the United States. J. Phys. Oceanogr. 12, 8-16.

Beckers, J. M., Rixen, M., 2003. EOF Calculations and Data Filling from Incomplete Oceanographic Datasets, J. Atmos. Ocean. Technol., 20(12), 1839–1856.

Chatterjee, A., Shankar, D., Shenoi, S.S.C., Reddy, G.V., Michael, G.S., Ravichandran, M., Gopalkrishna, V.V., Rao, E.P.R., Bhaskar, T.V.S.U., Sanjeevan, V.N., 2012. New atlas of temperature and salinity for North Indian Ocean. J. Earth Syst. Sci. 121 (3), 559–593.

Cook, T. M., Shay, L. K., 2002. Surface M2 tidal currents along the North Carolina shelf observed with a high-frequency radar. J. Geophys. Res. 107 (C12), 1-12.

Cosoli, S., Matjaz, L., Vodopivec, M., Malacic, V., 2013. Surface circulation in the Gulf of Trieste (northern Adriatic Sea) from radar, model, and ADCP comparisons. J. Geophys. Res. – Oceans, 118 (11), 6183-6200.

Dee, D. P., Uppala, S. M., Simmons, A. J., Berrisford, P., Poli, P., Kobayashi, S., et al., 2011. The ERA-Interim reanalysis: Configuration and performance of the data assimilation system. Q. J. Roy. Meteor. Soc. 137 (656), 553–597

Fernandes, A. A., Chandramohan, P., Nayak, B. U., 1993. Observed currents at Bombay High during a winter. Mahasagar, 26 (2), 95–104.

Ferrarin C, Tomasin A, Bajo M, Petrizzo A, Umgiesser G (2015) Tidal changes in a heavily modified coastal wetland. Cont Shelf Res 101: 22–33

Friedrichs, C. T., Aubrey, D. G., 1988. Non-linear tidal distortion in shallow well-mixed estuaries: a synthesis. Estuar. Coast. Shelf Sci. 27 (5), 521–545.

Friedrichs, C. T., Aubrey, D. G., 1994. Tidal propagation in strongly convergent channels. J. Geophys. Res. 99 (C2), 3321–3336.

Friedrichs, C. T., Madsen, O. S., 1992. Nonlinear diffusion of the tidal signal in frictionally dominated embayments J. Geophys. Res.: Oceans, 97 (C4), pp. 5637-5650

Giardino, A., Elias, E., Arunakumar, A., Karunakar, K., 2014. Tidal modelling in the Gulf of Khambhat based on a numerical and analytical approach. Indian J. Mar. Sci. 43 (7), 106-111.

Godin, G., 1983. On the predictability of currents. Int. Hydrographic Rev. 60, 119-126.

Gong, W. P., Schuttelaars, H., & Zhang, H. (2016). Tidal asymmetry in a funnel-shaped estuary with mixed semidiurnal tides. Ocean Dynamics, 66(5), 637–658. https://doi.org/10.1007/s10236-016-0943-1

Gough, M. K., Garfield, N., McPhee-Shaw, E., 2010. An analysis of HF radar measured surface currents to determine tidal, wind-forced, and seasonal circulation in the Gulf of the Farallones, California, United States. J. Geophys. Res. 15, C04019.

Guo, L. C., van der Wegen, M., Roelvink, J. A., He, Q. (2014). The role of river flow and tidal asymmetry on 1D estuarine morphodynamics. Journal of Geophysical Research: Earth Surface, 119, 2315–2334. https://doi.org/10.1002/2014JF003110

Jena, B. K., Arunraj, K. S., Suseentharan, V., Tushar, K., Karthikeyan, T., 2019. Indian Coastal Ocean Radar Network. Curr. Sci. 116, 372–378. doi: 10.18520/cs/v116/i3/372-378

Jena, B. K., Sivakholundu, K. M., Rajkmar, J., 2018. A description of tidal propagation in Hooghly estuary using numerical and analytical solutions. Ocean. Eng. 169, 38–48. doi: 10.1016/j.oceaneng.2018.09.009

Jithin, A. K., Unnikrishnan, A. S., Fernando, V., Subeesh, M. P., Fernandes, R., Khalap, S., Narayan, S., Agarvadekar, Y., Gankar, M., Tari, P., Kankonkar, A., Vernekar, S., 2017. Observed tidal currents on the continental shelf off the east coast of India. Cont. Shelf Res. 141, 51-67.

Kaplan, D. M., Lekien, F., 2007. Spatial interpolation and filtering of surface current data based on open-boundary modal analysis, J. Geophys. Res.-Oceans, 112, C12007, https://doi.org/10.1029/2006JC003984.

Kohonen, T., 1982. Self-Organized Formation of Topologically Correct Feature Maps, Biol. Cybern., 43, 59–69.

Kohonen, T., 1997. Self-Organizing Maps, 2nd edn., Springer, Heidelberg, Germany.

Kumar, S. S., Balaji, R., 2015. Effect of bottom friction on tidal hydrodynamics along Gulf of Khambhat. India. Estuar. Coast. Shelf Sci. 154, 129-136.

Kumar, V. S., Kumar, K. A., 2010. Waves and currents in tide dominated location off Dahej, Gulf of Khambhat, India. Mar. Geod. 33(2), 218–231.

Mandal, S., Sil, S., Shee, A., Venkatesan, R., 2018a. Upper Ocean and Subsurface Variability in the Bay of Bengal During Cyclone ROANU: A Synergistic View Using In Situ and Satellite Observations. Pure Appl. Geophys. 175 (12), 4605–4624. doi: 10.1007/s00024-018-1932-8

Mandal, S., Sil, S., Gangopadhyay, A., Murty, T., Swain, D., 2018b. On extracting high frequency tidal variability from HF radar data in the northwestern Bay of Bengal. J. Oper. Oceanogr. 11(2), 65-81.

Mandal, S., Sil, S., Shee, A., Swain, D., Pandey, P. C., 2018c. Comparative Analysis of SCATSat-1 Gridded Winds with buoys, ASCAT, and ECMWF winds in the Bay of Bengal. IEEE J. Sel. Top. Appl. Earth. Obs. Remote Sens. 11(3), 845-851.

Mandal, S., Pramanik, S., Sil, S., Arunraj, K.S., Jena, B.K., 2019a. Sub-mesoscale circulation features along the Andhra Pradesh Coast, Bay of Bengal: Observations from HF Radar. J. Coast. Res. 89 (accepted).

Mandal, S., Sil, S., Pramanik, S., Arunraj, K.S., Jena, B.K., 2019b. Characteristics and Evolution of a Coastal Mesoscale Eddy in the Western Bay of Bengal monitored by High-Frequency Radars. Dynam. Atmos. Oceans. 88, 101107. https://doi.org/10.1016/j.dynatmoce.2019.101107

Mandal, S., Pramanik, S., Halder, S., Sil, S., 2019c. Statistical analysis of coastal currents from HF radar along the North-Western Bay of Bengal. In: In: Murali, K.,Sriram, V., Samad, A., Saha, N. (Eds.), Proceedings of the Fourth International Conference in Ocean Engineering (ICOE 2018). Lecture Notes in Civil Engineering23. Springer, Singapore, pp. 89–97. https://doi.org/10.1007/978-981-13-3134-3_8

Murty, T. S., Henry, R. F., 1983. Tidal harmonics in the Bay of Bengal. J. Geophys. Res. 88(C10), 6069–6076.

Manoj, N. T.; Unnikrishnan, A. S., Sundar, D., 2009. Tidal asymmetry in the Mandovi and Zuari estuaries, the west coast of India. J. Coast. Res. 25 (6), 1187–1197.

Nayak, R. K., Shetye, S. R., 2003. Tides in the Gulf of Khambhat, west coast of India. Estuar. Coast. Shelf Sci. 57, 249–254.

Nayak, R. K., Salim, M., Mitra, D., Sridhar, P. N., Mohanty, P. C., Dadhwal, V. K., 2015.. Tidal and Residual Circulation in the Gulf of Khambhat and its Surrounding on the West Coast of India. J. Indian Soc. Remote. Sens. 43 (1): 151-162.

Nidzieko, N. J., 2010. Tidal asymmetry in estuaries with mixed semidiurnal/ diurnal tides. J Geophys Res 115, C08006. doi:10.1029/009JC005864

Nidzieko, N. J., Ralston, D. K., 2012. Tidal asymmetry and velocity skew over tidal flats and shallow channels within a macrotidal river delta. J Geophys Res 117, C03001. doi:10.1029/2011JC007384

Noble, M., Rosenfeld, L. K., Smith, R. L., Gardner, J. V., Beardsley, R. C., 1987. Tidal currents seaward of the northern California continental shelf. J. Geophys. Res. 92 (C2): 1733–1744.

Pawlowicz, R., Beardsley, B., Lentz, S., 2002. Classical tidal harmonic analysis including error estimates in MATLAB using T_TIDE. Computat. Geosci. 28 (8), 929–937.

Port, A., Gurgel, K. W., Staneva, J., Schulz-Stellenfleth, J., Stanev, E. V., 2011. Tidal and Wind-Driven Surface Currents in the German Bight: HFR Observations versus Model Simulations. Ocean Dyn. 61 (10), 1567-1585.

Pugh, D. T., 1987. Tides, Surges and Mean Sea-level, a handbook for engineers and scientists. John Wiley, New York.

Pugh, D.T., Woodsworth, P. L., 2014. Sea-level Science: Understanding Tides, Surges, Tsunamis and mean Sea-Level changes. Cambridge University Press, 407pp.

Shenoi, S. S. C., Antony, M. K., Sundar, D., 1988. Nature of the observed oscillatory flows in shelf waters of the western continental shelf of India, J. Coast. Res. 4 (4), 617–626.

Shenoi, S. S. C., Gouveia, A. D., Shetye, S. R., 1992. Diurnal and Semidiurnal tidal currents in the deep mid-Arabian sea. Proc. Indian Acad. Sci. (Earth Planet. Sci.). 101 (2), 177–189.

Shenoi, S. S. C., Gouveia, A. D., Shetye, S. R., 1994. M2 tidal currents on the shelf off Goa, West Coast of India, CSIR Golden Jubilee Symposium on Ocean Technology, 27-29 Aug 1992, NIO, Goa, Ocean Technology perspectives 1994, 415-427.

Shetye, S. R., Suresh, I., Shankar, D., Sundar, D., Jayakumar, S., Mehra, P., Desai, R. G. P., Pednekar, P. S., 2008. Observational evidence for remote forcing of the west India coastal current. J. Geophys. Res. – Oceans. 113, C11001.

Song, D., Wang, X. H., Kiss, A. E., Bao, X., 2011. The contribution to tidal asymmetry by different combinations of tidal constituents. J Geophys Res 116, C12007. doi:10.1029/2011JC007270

Speer, P. E., Aubrey, D. G., 1985. A study of non-linear tidal propagation in shallow inlet/estuarine systems. Part II: Theory. Estuar. Coast. Shelf Sci. 21 (2), 207–224.

Subeesh, M. P., Unnikrishnan, A. S., Fernando, V., Agarwadekar, Y., Khalap, S. T., Satelkar, N. P., Shenoi, S. S. C., 2013. Observed tidal currents on the continental shelf off the west coast of India. Cont. Shelf Res. 69, 123–140.

Subeesh, M. P., Unnikrishnan, A. S., 2016. Observed internal tides and near-inertial waves on the continental shelf and slope off Jaigarh, central west coast of India. J. Marine Syst. 157, 1-19.

Suh, S. W., Lee, H. Y., Kim, H. J., 2014. Spatio-temporal variability of tidal asymmetry due to multiple coastal constructions along the west coast of Korea. Estuar. Coast. Shelf. Sci. 151:336–346

Testut L. Unnikrishnan A.S., 2016. Improving Modeling of Tides on the Continental Shelf off the West Coast of India. J. Coast. Res. 32 (1), 105 – 115.

Unnikrishnan, A. S., Antony, M. K., 1990. On vertical velocity fluctuations and internal tides in an upwelling region off the west coast of India. Estuar. Coast. Shelf Sci. 31, 865–873.

Unnikrishnan, A. S., Shetye, S. R., Michael, G. S. 1999a. Tidal propagation in the Gulf of Khambhat, Bombay High and surrounding areas. Proc. Indian Acad. Sci. (Earth Planet. Sci.). 108, 155–177.

Unnikrishnan, A. S., Gouveia A. D., Vethamony, P. 1999b. Tidal regime in Gulf of Kutch, west coast of India, by 2D model. J. Waterway, Port, Coastal, Ocean Eng. 125 (6), 276–284.

Varkey, M. J. 1980. Power spectra of currents off Bombay. Indian J. Mar. Sci. 9, 278–280.

Wang, Z. B., Juken, H., & de Vriend, H. J. (1999). Tidal asymmetry and residual sediment transport in estuaries. WL/Hydraulic, report No. Z2749, 66 pp

Xu, H., Wolanski, E., Chen, Z. 2013. Suspended particulate matter affects the nutrients budget of turbid estuaries: modification of the LOICZ model and application to the Yangtze Estuary. Estuar. Coast. Shelf Sci. 127, 59–62.

Appendices

A. QA/QC of HFR data

The inbuilt real-time QA/QC procedures adapted by ICORN (Jena et al., 2019), are the same as those followed by the Integrated Ocean Observing System (IOOS) of the National Oceanic and Atmospheric Administration (NOAA). These radars are of direction-finding type, consisting of a receiving and transmitting antennae at each location. The measurements of the HFR echoes backscattered from the sea surface are used to deduce information on both waves and surface currents (Barrick et al., 1977). The entire QA/QC procedure, usually applied on the HFR-derived currents, has three steps: (i) the signal-processing step (i.e., the investigation of Doppler spectra), (ii) the development of radial components, and finally, (iii) the development of total vector components of surface currents, which required two overlapping nearby sites. The Doppler spectra QC tests (consisting of 17 tests, mainly, the noise floor detection and computation, first-order Bragg peak detection and measurements, detection and removal of burst interference, ionospheric and ship echoes, etc.) are already embedded in the acquisition system. The radial velocities will not be produced if the QC test on the Doppler spectra fails. The antenna calibration, also known as antenna pattern measurement (APM), is vital in ensuring the accuracy of surface current measurements. During the development of radial components, QC is performed on several technical parameters, namely, the antennae pattern type, site code, site coordinates, threshold values of radial velocity (site specific) and time zone.

For the development of total surface currents, radial mapping from at least two sites (Jegri and Wasi lighthouses) is a must (Barrick et al., 1977). The antennae pattern type is ideal, with a threshold radial velocity at Jegri and Wasi Borsi of 2.55 m s^{-1} each. The ICORN maintain a radar wavelength of 68 m at GoKh. The essential tests consist of maintaining the data density threshold (sufficient number of radial velocities should exist to compute a total velocity vector), maximum total speed threshold and maximum Geometric Dilution of Precision (GDOP) threshold. Along the Gulf, the HFRs operates with a GDOP of 20, with a threshold total speed limit up to 2.50 m s^{-1}, and measure's currents at a spatial resolution of ~6 km every hour.

B. Statistical Analysis of the HFR Surface Currents

The hourly time series along the western part of Gulf at location W shows that the zonal and meridional components vary from -1.18 to 0.88 m s^{-1} and -1.76 to 1.11 m s^{-1} respectively, along with two spring and neap tides. The maximum current speed of ~2.0 (1.5) m s^{-1} is observed during spring (neap)

tide (Fig. B.1a). The mean zonal (-0.13 m s^{-1}) and meridional (-0.17 m s^{-1}) currents are negative, indicating south-westward flow during the period of study. The standard deviation (SD) at location W shows a higher value for the zonal currents (0.52 m s^{-1}) than that of meridional currents (0.44 m s^{-1}). The boxplot shows extreme values (outliers) for meridional currents with medians -0.20 m s^{-1}; however, no outliers are observed for the zonal currents (Figs. B.1b and B.1c). The interquartile range (IQR) is -0.66 – 0.33 (-0.46 – 0.26) m s^{-1} for the u (v) component, indicating more variability in the meridional component (Figs. B.1b and B.1c). The boxplot shows the presence of outliers (3*IQR), but the data shows symmetric behaviour about the median. Also, students' t-test indicates that the HFR datasets are 95% significant (Mandal et al., 2018b).

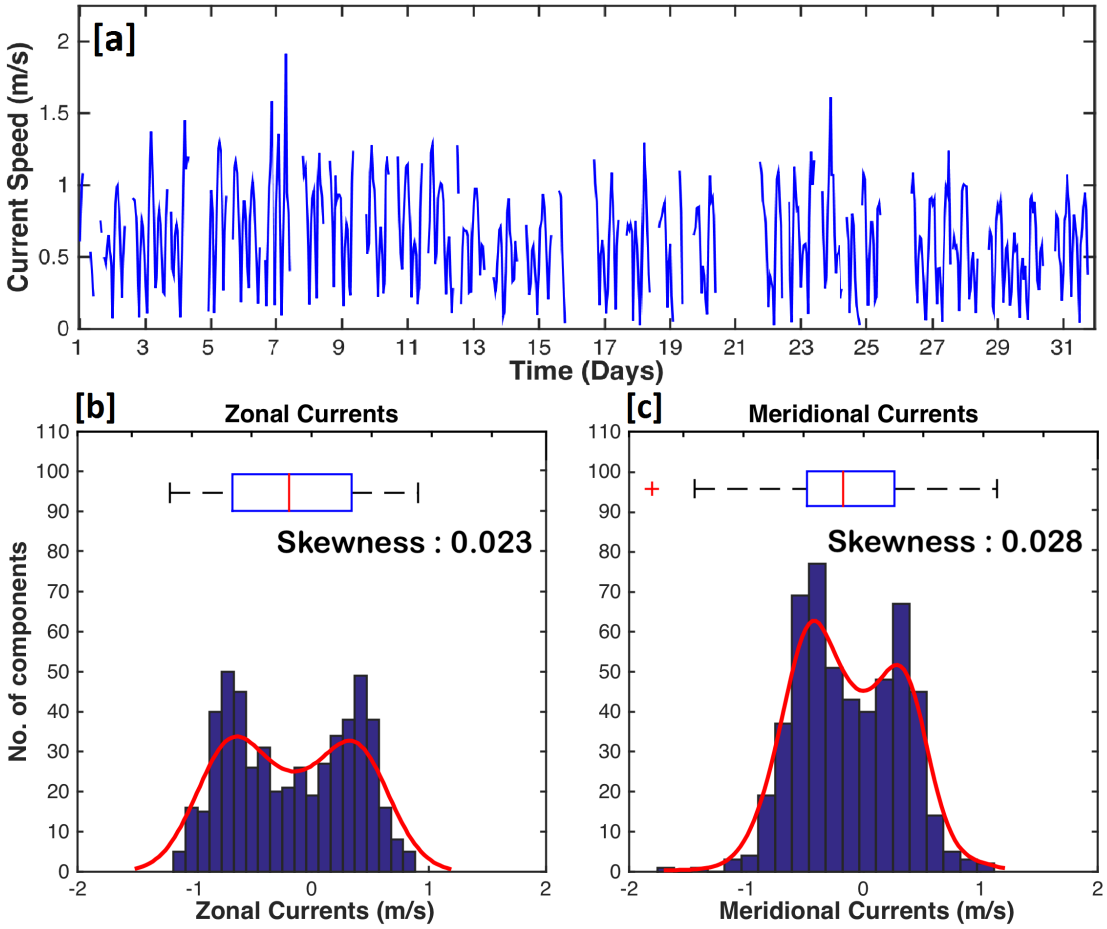

Fig. B.1: (a) The hourly variation of current magnitude (in m s^{-1}) at location W. The probability density functions for (b) zonal currents (m s^{-1}) and (c) meridional currents (m s^{-1}) at location W. The boxplots corresponding to both components are incorporated. The red line in the middle of the box is the median. The upper (lower) end of the boxplot indicates the third (first) quartile. The red '+' symbol indicates outliers.

Both the zonal and meridional currents follow bimodal distribution (Figs. B.1b and B.1c) to indicate the presence of both high and low tides throughout the data (curved red line). Positive skewness of 0.023 and 0.028 is also observed for the zonal and meridional components, respectively. Also, higher variability is observed for the meridional current, which is well comparable to the higher variability from the boxplot and distribution curves indicating dominant currents variability in the north-south direction (Figs. B.1b and B.1c) (Unnikrishnan et al., 1999b). The extreme outliers observed from boxplot of meridional HFR current can also be seen in the distribution curve.